(2)

AD

Rapid Annealing of Ion Implanted $Hg_{1-x}Cd_xTe$

Final Technical Report

by

Prof. Rafael Kalish

March 1990

RYD 5231-EE-01

United States Army
European Research Office of The U.S. Army
London England

Contract Number: DAJA45-86-C-0011
Technion Research & Development Fundation, LTD

AD

Rapid Annealing of Ion Implanted $Hg_{1-x}Cd_xTe$

Final Technical Report

by

Prof. Rafael Kalish

March 1990

United States Army

European Research Office of The U.S. Army

London England

Contract Number: DAJA45-86-C-0011

Technion Research & Development Fundation, LTD

SECURITY CLASSIFICATION OF THIS PAGE (When Data Entered)

REPORT DOCUMENTATION PAGE		READ INSTRUCTIONS BEFORE COMPLETING FORM
1. REPORT NUMBER	2. GOVT ACCESSION NO.	3. RECIPIENT'S CATALOG NUMBER
4. TITLE (and Subtitle) RAPID ANNEALING OF ION IMPLANTED $Hg_{1-x}Cd_xTe$		5. TYPE OF REPORT & PERIOD COVERED Final Report 1.10.86-28.2.90
		6. PERFORMING ORG. REPORT NUMBER
7. AUTHOR(s) Rafael Kalish		8. CONTRACT OR GRANT NUMBER(s) DAJA45-86-C-0011
9. PERFORMING ORGANIZATION NAME AND ADDRESS Mr. F. Naggar, Technion Research & Development Foundation LTD.		10. PROGRAM ELEMENT, PROJECT, TASK AREA & WORK UNIT NUMBERS
11. CONTROLLING OFFICE NAME AND ADDRESS Technion-Israel Institute of Technology Haifa 32 000, Israel		12. REPORT DATE March 1990
		13. NUMBER OF PAGES
14. MONITORING AGENCY NAME & ADDRESS (if different from Controlling Office) European Office of the US Army London		15. SECURITY CLASS. (of this report)
		15a. DECLASSIFICATION/DOWNGRADING SCHEDULE

16. DISTRIBUTION STATEMENT (of this Report)

17. DISTRIBUTION STATEMENT (of the abstract entered in Block 20, if different from Report)

18. SUPPLEMENTARY NOTES Partially published in:
APL 51, 1158(1987); NIM B35, 319(1988); APL 55, 1091(1989);
J. Cryst. Growth 86, 744(1988); J. Vac. Sci. & Technol A7, 2575 (1989).

19. KEY WORDS (Continue on reverse side if necessary and identify by block number)

$Hg_{1-x}Cd_xTe$, ion implantation, damage annealing, stoichiometry, electrical properties. (MCT)

20. ABSTRACT (Continue on reverse side if necessary and identify by block number)

Different Rapid Thermal Annealing techniques have been employed to achieve damage removal and electrical activation of dopants in ion implanted $Hg_{1-x}Cd_xTe$ ($x=0.2, 0.3$). As seen by Rutherford Backscattering Spectrometry combined with channeling and Auger measurements annealings with a CO_2 laser or a flash lamp

DD FORM 1 JAN 73 1473 EDITION OF 1 NOV 65 IS OBSOLETE

SECURITY CLASSIFICATION OF THIS PAGE (When Data Entered)

lead to good removal of implantation damage without causing changes in the stoichiometry. These techniques, however, suffer from complexity and lack of reproducibility. The new simple method for RTA of mercury containing crystals , Annealing by immersion in a hot MErcury BAth (AMEBA) which we have developed within the present project was found to be comparable to other more complicated techniques as for improving the electrical properties of HgCdTe as deduced from Hall and differential Hall measurements. The conductivity of as recrystallized p type samples can be converted to n type with a low carrier concentration and a high mobility; The mobility of n-type samples can be increased following immersion annealing in a hot Hg bath and B implants can be electrically activated by this simple technique.

Table of Contents

1. Statement of the problem and background

$Hg_{1-x}Cd_xTe$ (with x=0.2; 0.3), is presently the most widely used semiconductor for the fabrication of infrared detectors. Its band gap can be tailored to cover the two atmospheric windows for Infra Red radiation, 3-5 μm and 8-14 μm respectively. The doping of this material is, however, complicated by the fact that its electrical properties are determined by defects and deviations from stoichiometry and not only by electrically active impurities. For example, as grown HgCdTe is usually Hg vacancy rich and therefore presents a high p type conductivity with low mobility.

Ion implantation, a well established technique for controled doping of semiconductors leads, when applied to HgCdTe, to the formation of an n^+ layer which penetrates a few microns into the crystal and is attributed to electrically active implantation induced damage [1-2]. The fact that the damage itself is n type, is utilized in most infrared devices fabricated in $Hg_{1-x}Cd_xTe$ (x=0.2, 0.3) up to date. In these, however, the advantages of the control of the junction depth and electrical profile which implantation doping can offer, are clearly lost. Several successful attemps to anneal out the radiation damage and to achieve real chemical doping in HgCdTe have been reported in the last few years [3-6]. The difficulties encountered in the annealing of MCT stem from the tendency of the material to lose Hg upon heating which alters its stoictiometry and electrical properties. Hence the necessity of performing the post implantation annealing either under an overpressure of Hg or on encapsulated samples.

In our proposal we have suggested to utilize rapid annealing techniques, which have the advantages of heating the sample up to temperatures close to the melting point for short times (a few seconds), as under such conditions minimal stoichiometric changes may be expected. The first method for obtaining rapid heating was by exposing the sample to short pulses from a CO_2 laser. In a serie of publications (7-9) we have shown that this annealing, when applied to HgCdTe (x=0.3), removes the implantation damage and activates the implants without causing changes in the stoichiometry. P/n photodiodes were produced by activation of P implants in HgCdTe x=0.29 annealed by a single 0.4 sec pulse from a CO_2 laser. Our first objective was to perfect this technnique in order to obtain, in a more reproduceable way p on n diodes in HgCdTe (x=0.3) and to extend it to the narrower band gap HgCdTe (x=0.2). The second technique we have proposed was to achieve Rapid Thermal Annealing (RTA) by subjecting the samples to intense light in a flash lamp ("HEATPULSE") instrument. This technique has proven to be very efficient for the annealing of other compound materials for which one of the components has a high vapor pressure (GaAs, InP, CdTe...). Therefore, we have planned to adapt the R.T.A. technique to $Hg_{1-x}Cd_xTe$ i.e. to find the optimum experimental conditions (time, temperature, cap) to achieve removal of implantation damage and activation of the dopants. The next section describes the work carried out on CO_2 laser annealing and heatpulse annealing and presents a new and very promissing annealing method : "Annealing by immersion in a hot MErcury BAth (AMEBA)" developed by us in the course of the present research, and which is an alternative RTA method particularly suitable for the annealing of Hg containing crystals.

2. Results and discussions

2.1. Development work on the CO_2 laser annealing

In our previous studies of CO_2 laser annealing of $Hg_{1-x}Cd_xTe$(x=0.3), we have encountered some difficulties in measuring the sample temperature and maintaining a uniform temperature on the specimen surface. In the improved arrangement a beam homogenizer consisting of a simple rectangular cavity made of four polished stainless steel plates was added to avoid "hot spots" on the sample surface during CO_2 laser irradiation. The temperature uniformity was also achieved by using indirect heating of the implanted surface by exposing a quartz plate , in good contact with the sample, to the photons from the CO_2 laser. The quartz served both as an absorbing medium, a temperature diffuser and a proximity cap for the specimen. Steady state temperatures could be obtained by the simultaneous heating the sample by the laser and its cooling by a jet of N_2 gas. Because of the rareness of MCT samples we have performed the experiments on InSb, an IR material which also tends to change stoichiometry upon heating. In ref. [1C] (see enclosed) , we have shown that good annealing of ion implanted InSb can be achieved with this arrangement. The annealing quality, as determined from RBS measurements, was comparable to that obtained by furnace annealing. Auger electron spectroscopy was used to check whether the CO_2 laser annealing has caused major changes in the near surface stoichiometry. The results have shown that only the topmost 200A have been affected by the annealing procedure.

Nevertheless, this method suffers from two difficulties: 1) The determination of the real sample surface temperature is problematic because it depends on the thermal contact with the quartz plate. 2) The annealing reproducibility is hard to obtain because of inherent variation in laser output.

2.2. Flash Lamp Rapid Thermal Annealing:

The "Heatpulse" instrument available at the Technion for Rapid Thermal processing was a multiuser system; hence its contamination by Hg or other volatile materials which may be evaporated during Rapid Thermal Annealing Experiments was highly undesirable. In order to enable the enclosure of the samples during processing, two boxes, fitting into the Heatpulse instrument, have been constructed, one made of high purity graphite and the other of quartz. Both have been tested on Si samples with thermocouples glued onto them. The thermal response of the quartz box seems superior to that made of graphite. The sample to be annealed was placed on a Si wafer onto which a thermocouple had been glued. Because of the small heat capacity of the sample arrangement, fast rise times of the sample temperature could be obtained. Using the Heatpulse in the "power mode", good control of the sample temperature in the required range of 300-400C could be obtained. We have shown that Heatpulse annealing performed at 400C for 10s totaly removes the damage created by implantation in InSb as seen by R.B.S. experiments [10].

These first annealing experiments carried out with a CO_2 laser or with a Heatpulse yielded some promissing preliminary results with regard to the removal of ion implantation damage. However, these techniques suffer from a lack of reproducibility and accuracy of the experimental conditions (time, temperature). The need to combine, in a single annealing technique, well defined temperature and time and a Hg atmosphere has led us to the development of a new simple annealing technique which fulfils these requirements, Annealing by immersion in a hot Mercury Bath (AMEBA), hence the deviation from the original proposal.

2.3 Development of a new annealing method: Annealing by immersion in a hot Hg Bath (AMEBA).

2.3.1. Presentation of the AMEBA

We have developed a new simple annealing technique which doesn't require any encapsulation yet is performed in a Hg rich atmosphere. The main idea is to dip the sample to be annealed in a hot Hg bath in such a way that it will experience the temperature of the liquid for the well known immersion time, will be in a Hg rich atmosphere, yet not in contact with the liquid itself. In a preliminary version, the sample was sandwitched between two Si wafers and immersed in the bath, the temperature of which was controlled by a thermocouple connected to a temperature controller. It turned out, from Hall effect measurements, that following the initial AMEBA, the sample showed strong n type conductivity.

This phenomenon was found to be associated with a wetting of the sample periphery by liquid Hg. To overcome this problem the sample, sandwiched between the two Si platelets, was placed in a small box (first made of graphite and finaly of stainless steel) the dimensions of which fit tightly those of the Si platelets. The box was closed by a lid with a fine thread which pressed gently on the whole assembly allowing Hg vapor to penatrate but preventing any direct wetting of the sample. This simple method permits annealings at well defined temperatures (below the boiling point of Hg) and times (from a few seconds to a few hours) in a Hg rich atmosphere.

2.3.2. Performances of the AMEBA

2.3.2.1 Removal of ion implantation induced damage

Ion beam probing techniques, Rutherford backscattering combined with channeling and Proton Induced x-rays emission, were utilized to check the near surface crystalline quality and stoichiometry of ion implanted and immersion annealed $Hg_{1-x}Cd_xTe$. After a 30 s AMEBA at 260C, the reduction of the damage induced by In implantation in $Hg_{1-x}Cd_xTe$ ($x=0.23$) was found to be comparable to that obtain with classical thermal annealing in an ampoule. Under such conditions no noticeable change in stoichiometry, as determined by

measuring the characteristic x-rays excited by low energy was protons could be detected [11-12] (see enclosed).

2.3.2.2. Improvement of the electrical properties of as-grown and ion implanted HgCdTe.

We have investigated the AMEBA with regard to improving the electrical properties of as-grown and ion implanted samples. Using Hall and differential Hall measurements we have shown that this technique is comparable to other, more complicated, annealing techniques as for improving the electrical properties of $Hg_{1-x}Cd_xTe$ (x=0.21) samples. As - recrystalized p type samples can be converted to good n type ($\mu=10^5 cm^2 s^{-1}$, $n=10^{14} cm^{-3}$) following AMEBA at 260°C for 30n. This annealing, when performed at 250C for a few minutes improves the mobility of undoped n type samples by as much as 50%. Electrical activation of B implants in $Hg_{0.79}Cd_{0.21}Te$ can be achieved following immersion for 8' in the Hg bath at 320C[13.14]. (see enclosed).

2.4. Understanding the damage in $Hg_{1-x}Cd_xTe$(Various x).

As we have pointed out in the introduction, the n type layer used in the $Hg_{1-x}Cd_xTe$ (x=0.2, 0.3) infrared detectors is realized by ion implantation induced damage, in which case the electrical properties are governed by the damage rather than by impurity doping. Interestingly, the doping effects due to

the damage extend much deeper into the crystal than the range of the implants showing that the damage related donor states can not be directly associated with simple point defects.

Recently, we have shown that Ar,Xe and In implantations in $Hg_{1-x}Cd_xTe$ (x=0.7, Eg=0.9eV which is suitable for optical fiber communication at 1.3μm) have turned the material highly resistive[15]. The study of the nature of implantation induced damage in $Hg_{1-x}Cd_xTe$ for various x and for In and B ions is of importance because of the use made of the damage as a doping mechanism. It is however also of basic interest due to the changes that the material undergoes with x (bond strengh, bond length, ionicity..). For this, the build-up of damage induced by In or B implantations into $Hg_{1-x}Cd_xTe$ for various x (x=0, x=0.25, x=0.4, x=0.7, x=1) was measured by means of Channeling Rutherfored backscattering spectroscopy (RBS). It was found that for room temperature implantation the damage was always in the form of extended defects. Damage profiles were extracted using a model based on Quere's dechanneling treatment. Despite the large difference in bond nature and related physical properties between the different compositions, the general trend in damage formation was found to be similar for all x values studied, though displaced by up to two orders of magnitude in dose, HgTe damaging much easer than CdTe [16] (see enclosed).

The transition upon heating from point defects, frozen-in for low temperature implantation in $Hg_{1-x}Cd_xTe$ (x=0.24) , to extended defects has been monitored through ion-channeling experiments in the temperature range

100-360K. It was found that defects formed by the agglomeration of frozen-in point defects are confined to a depth which roughly corresponds to the implant range, in constrast to defects directly created by room temperature implantation which extend much deeper into the crystals [17] (see enclosed).

2.5. Experiments on $Hg_{1-x}Cd_xTe$ epitaxial layers

Recently, we have received from Dr.J. Dinan of the Night Vision and Electro-optic Army Labs at Fort Belvoir a few electrically uncharacterized $Hg_{1-x}Cd_xTe$ ($x=0.25$) epilayers grown by the close-spaced Vapor Phase Epitaxy technique. The Hall effect characterization, following a slight etch, showed that some of the samples could not be measured, probably due to the presence of n type islands scattered in the p type layer. The measureable samples(sample# 120584) which presented good p type conductivity ($P_{77k}=1.6\ 10^{16}cm^{-3}$ and $\mu\rho_{77K}=420\ cm^2V^{-1}S^{-1}$), where used to check the feasability of the AMEBA on epilayers. Electrical activation of B implants was achieved following AMEBA performed under conditions identical to those used for bulk HgCdTe (352C, 8'), as seen by Hall effect measurements. The possibility that the observed behaviour is not due to electrical activity of B implants but is related to the implantation damage or to the immersion procedure was eliminated by performing the same annealing on Ne-implanted and non implanted samples (see results in table 1).

Conclusion

Short time annealing of implanted HgCdTe (x=0.2, 0.3) was shown to electrically activate B implants in p-type material. Particularly promising is the novel annealing technique developed within the present research in which defect removal and electrical activation are obtained by immersion of the implanted sample in a hot mercury bath (AMEBA). This technique, which is extremely simple and inexpensive, consistently activated B implants and improved the n-type properties of both n and p (vacancy/grown material. It would be most desirable to continue the studies on the AMEBA technique and its implementation in achieving also p-type conductivities and IR sensitive PV devices in ion implanted and annealed HgCdTe.

References

1. L.O. Bubulac, W.E. Tennant, S.H. Shin, C.C. Wang, M. Lanir, E.R. Gertner, and E.D. Marshall. Jap. J. Appl. Phys. 19, 495(1980).
2. G.L. Destefanis, Nucl. Instrum. Methods 209, 210, 567(1983).
3. L.O. Bubulac, D.S. Lo, W.E. Tennant, D.D. Edwall, J.C. Chen, J. Ratusnik, J.C. Robinson and G. Bostrup Appl. Phys. Lett. 50, 1586(1987).
4. G.L. Destefanis, J. Cryst. Growth 86, 700(1987).
5. T.M. Kao and T.W. Sigmon Appl. Phys.Lett. 41, 1057(1982).
6. L.O. Bubulac, J. Cryst. Growth 86, 723(1987).
7. G. Bahir and R. Kalish, J. Appl. Phys. 54, 3129(1983).
8. G. Bahir and R. Kalish, Appl. Phys.Lett. 41, 1057 (1982).
9. R. Kalish, J. Cryst. Growth 72, 474 (1985).
10. U. Neta, V. Richter and R. Kalish, MRS Anaheim .
11. R. Kalish, R. Fastow, V. Richter and M. Shaanan, Appl. Phys. Lett. 51, 1158 (1987).
12. M. Shaanan , V. Richter and R. Kalish,Nucl. Instr.Meth. B35, 319(1988).
13. C. Uzan-Saguy and R. Kalish, Appl. Phys.Lett. 55, 1091(1989).
14. C. Uzan-Saguy, D. Laser and R. Kalish, in J. Cryst. Growth in press.
15. C. Uzan, Y. Marfaing, R. Legros, R. Kalish and V. Richter, J. Cryst. Growth 86,744(1988).
16. C. Uzan-Saguy, D. Comedi, V. Richter and R. Kalish, J. Vac.Sci. Technol. A7, 2575(1989).
17. V. Richter and R. Kalish, in press.

Table 1

Electrical properties of B and Ne implanted and AMEBA treated epi layers measured at (B=2000G, LN_2 temperature)

	Type	carrrier concentration cm^{-3} [Thickness]	mobility $cm^2V^{-1}s^{-1}$
As etched	p	$1.5x10^{16}$ [13μ]	420
B implanted $10^{14}cm^{-2}$; 200keV	n	$1x10^{18}$ [1μ]	5370
Ne implanted $3x10^{13}cm^{-2}$,320keV	n	$1x10^{18}$ [1μ]	3100
B annealed 10', 325C	n	$3x10^{17}$ [1μ]	22000
Ne annealed 10' 325C	indetermined		
Ne annealed 20' 325C	p	$4x10^{17}$ [13μ]	112
non implanted annealed 20',325C	n	$2.4\ 10^{17}$ [1μ]	1200
non implanted annealed 20', 325C etched ~1μ	p	$7x10^{16}$ [12μ]	200

List of publications that have received supported from ERO

1. U. Neta, V. Richter and R. Kalish, MRS Anaheim.
2. R. Kalish, R. Fastow, V. Richter and M. Shaanan, Appl. Phys. Lett. 51, 1158 (1987).
3. M. Shaanan, V. Richter and R. Kalish, Nucl. Instr. Meth.B35, 319(1988).
4. C. Uzan-Saguy and R. Kalish, Appl. Phys. Lett. 55, 109(1989).
5. C. Uzan-Saguy, D. Laser and R. Kalish, in press in J. Cryst. Growth.
6. C. Uzan, Y. Marfaing,R. Legros, R. Kalish and V. Richter , J. Cryst. Growth 86, 744 (1988).
7. C. Uzan-Saguy, D. Comedi, V. Richter and R. Kalish, J. Vac. Sci. Technol.A7, 2575 (1989).
8. V. Richter and R. Kalish, in press in J. Appl. Phys.

Electrical activation of B implants in $Hg_{0.79}Cd_{0.21}Te$ by immersion annealing in a hot Hg bath

C. Uzan-Saguy and R. Kalish
Department of Physics and Solid State Institute, Technion–Israel Institute of Technology, Haifa 32 000, Israel

(Received 19 April 1989; accepted for publication 5 July 1989)

Electrical activation of B implants in $Hg_{0.79}Cd_{0.21}Te$ was achieved following annealing by immersion in a hot Hg bath at 320 °C for 8 min. Annealing of the implantation damage and partial electrical activation was obtained after such treatment as deduced from Rutherford backscattering combined with channeling and differential Hall measurements. The possibility that the observed behavior is not due to electrical activity of the B implants but is related to the implantation damage or to the immersion procedure was eliminated by control experiments on Ne-implanted and on nonimplanted samples.

The removal of implantation-related damage in $Hg_{1-x}Cd_xTe$ and the electrical activation of the implants are complicated in this delicate material by the tendency of the damage to form relatively stable complexes, and by the ease of formation of stoichiometric defects. The damage itself is known to be *n* type, a fact which is being utilized in most infrared devices fabricated in HgCdTe up to date, which are based on *n*(damage)-on-*p* structures. Nevertheless, several successful attempts to achieve real chemical doping in HgCdTe have been reported over the last few years.[1–7] In these, post-implantation annealing was performed at different times and temperatures in either a saturated Hg overpressure or on encapsulated samples. Recently we have reported[8] on a new, extremely simple, annealing procedure which does not require encapsulation, is carried out in a Hg-rich atmosphere, and enables very good control on the annealing temperature and time. In this technique, ion-implanted HgCdTe is sandwiched between two flat clean surfaces (i.e., Si) and is immersed for a given time in a liquid-mercury bath held at the required temperature. By employing ion beam probing techniques [Rutherford backscattering spectrometry (RBS) and proton-induced x-ray emission (PIXE)] we have shown[8] that good near-surface crystal quality (i.e., damage removal) and stoichiometry (i.e., no Hg loss) could be achieved by this immersion annealing technique. In the present work we report on successful electrical activation of B implants in HgCdTe obtained by the above annealing method.

The experimental setup described in Ref. 8 was substantially improved; the major change being that the sample is now placed in a small stainless-steel box, the dimensions of which fit tightly those of the two Si proximity caps. A lid with a fine thread enables closing the box while gently pressing down on the assembly in a way which prevents any wetting of the sample but allows the penetration of Hg vapor when immersed in the liquid. The whole assembly is placed inside a well-vented hood. Four different experiments were carried out in order to eliminate any possible spurious effects which may be related to the implantation-induced damage or to the immersion procedure:

(i) A *p*-type $Hg_{0.79}Cd_{0.21}Te$ single crystal oriented in the (111) direction has been implanted at room temperature with 200 keV boron ions to a dose of 1×10^{14} cm^{-2}, keeping the beam current below 30 nA/cm^2 to avoid sample heating during implantation. The implanted sample has been immersion annealed for 8 min at 320 °C. RBS channeling experiments, using 320 keV protons, were employed to assess the implantation damage and its removal by the annealing procedure. Figure 1 shows the RBS spectra obtained for the sample at its unimplanted, implanted, and annealed stages. A random spectrum taken under nonchanneling conditions is also shown. It is evident from the figure that within the sensitivity limit of the channeling technique, the annealing has effectively removed all implantation-related damage as the annealed channeling spectrum coincides with that of the virgin crystal. The present immersion annealing technique can also lead to substantial improvements of both crystallographic and electric properties of as-grown $Hg_{0.79}Cd_{0.21}Te$; however, this work will be reported elsewhere.[9]

(ii) One-half of a *p*-type As-doped $Hg_{0.79}Cd_{0.21}Te$ sample has been B implanted and immersion annealed under conditions identical to those of (i) above. The electrical properties of the unimplanted, implanted, and annealed sample have been determined from van der Pauw Hall measurements at 77 K in a magnetic field of 2 kG. The results are given in Table I. As is evident from the table, the annealing has reduced the donor carrier concentration by a factor of

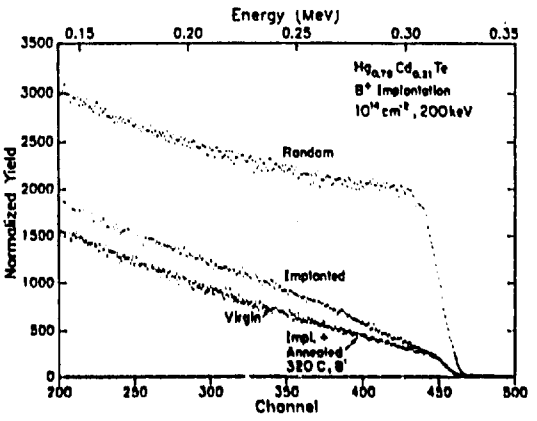

FIG. 1. Channeling Rutherford backscattering spectra obtained in $Hg_{0.79}Cd_{0.21}Te$ with 320 keV protons showing the virgin, B-implanted, and immersion-annealed spectra. A random spectrum is also displayed.

 0003-6951/89/371091-03$01.00

TABLE I. Mobility and carrier concentration obtained for $Hg_{1-x}Cd_xTe$: (I) B/Ne-implanted samples before and after immersion annealing (320 °C, 8'). (II) Virgin sample before and after immersion annealing (320 °C, 8').

Sample	Impl. ion	Anneal 320 °C 8'	Cond. type	Mobility ($cm^2 V^{-1} s^{-1}$)	Carriers conc (cm^{-3})
I	···	no	p	600	6×10^{15}
I	B	no	n	3 000	2×10^{16} [a]
I	Ne	no	n	3 000	2×10^{16} [a]
I	B	yes	n	28 000[b]	1×10^{17} [a]
I	Ne	yes	p	70	2×10^{16}
II	···	no	p	450	1×10^{16}
II	···	yes	p	200	4×10^{16}

[a] Deduced for a thickness of 1 μm.
[b] This mobility was measured at a depth of 1.2 μm. Prior to any etching the measured mobility was 20 000 $cm^2 V^{-1} s^{-1}$.

about 20, while increasing the mobility by about an order of magnitude (to 28 000 $cm^2 V^{-1} s^{-1}$), indicating that some chemical doping was achieved by the thermal treatment. Differential Hall measurements, performed by controlled etching of the sample in a calibrated dilute bromine in methanol solution, have shown that the carrier concentration peaks at a depth of 5000 Å, the junction being located about 1.5 μm below the surface (see Fig. 2).

(iii) The second half of the same wafer as used for the B implantation of (ii) above has been implanted with 320 keV Ne ions to a dose of 3×10^{13} cm^{-2}. The dose and energy for this implantation have been chosen such[10] that the amount of damage and its profile coincide with those caused by the B implantation. The Ne-implanted sample has been annealed together with the B-implanted one, both having been placed side by side in the annealing "box" that was immersed in the hot Hg bath. The results of Hall measurements following the implantation and annealing of the Ne-implanted sample are also given in the table. The marked difference between the B- and Ne-implanted and annealed samples is evident: while as a result of the implantation, both B and Ne samples exhibited identical *n*-type conductivities attributed to radiation damage, their electrical properties were drastically different following the annealing. The Ne (a nondopant noble gas) implanted sample has returned *p* type with a very poor mobility while its B (a donor) implanted "twin" sample exhibited a clear *n*-type conductivity with a rather high mobility. The poor hole mobility and high carrier concentration measured for the Ne-implanted and annealed sample may be indicative of mixed conduction, possibly caused by donor activity due to some residual noncompletely annealed damage.

(iv) A sample cut from the same ingot as used for the previous studies has been exposed, without any implantation, to an identical immersion annealing procedure and its electrical properties have been measured (see Table I, sample II). In contrast to the implanted samples, this virgin sample has remained *p* type after annealing with a somewhat reduced mobility, indicative for mixed conduction, possibly due to a thin *n*-type layer formed on the crystal surface. Indeed, careful differential Hall measurements have shown that bulk properties were reached already after etching of about 1000 Å, in sharp contrast to the strong and deeply extending *n*-type behavior found for the B-implanted and annealed sample.

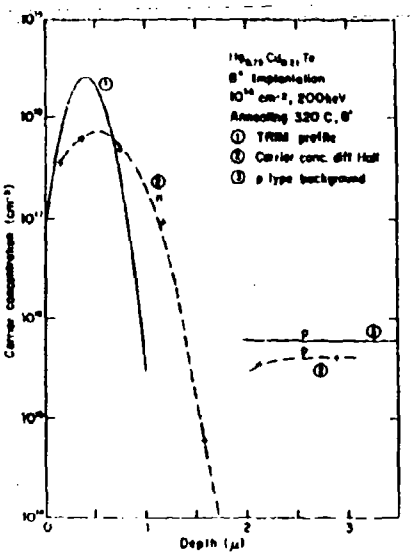

FIG. 2. Electrical conductivity profile as deduced from differential Hall measurements on $Hg_{1-x}Cd_xTe$ implanted with B (10^{14} cm^{-2}, 200 keV) and immersion annealed for 8' at 320 °C. The calculated profile for this case is shown for comparison.

We have conclusively demonstrated that the newly developed immersion annealing technique yields *n*-type conductivities which must be directly related to B implants in HgCdTe. This was verified by carrying out control experiments on identically annealed samples which were either nondamaged or purely damaged by the implantation of nondopant ions. These, when annealed, have shown electrical properties markedly different from those found for the B-implanted sample. The depth profile found for the donor activity in the case of B implantation is deeper than the expected implant profile deduced from range calculations[10] (see TRIM profile in Fig. 2). Since it is known from secondary-ion mass spectroscopy measurements[11,12] that B does not substantially diffuse in HgCdTe at the temperatures and times relevant to the present experiment, we find support in the present *n*-type profile to the explanation offered by Bubulac[13] that deep donor activities can be attributed to boron-related complexes and possibly to a channeling tail, which extends deeper into the crystal than the calculated B profile.

The authors would like to thank Dr. R. Eastow for help and discussions and Dr. Richter for assistance in the ion implantation and Rutherford backscattering experiments. This research was supported in part by the U.S. Army contract No. DAJA45-86-C-0011.

[13] L. O. Bubulac, D. S. Lo, W. E. Tennant, D. D. Edwall, J. C. Chen, J. Ratusnik, J. C. Robinson, and G. Bostrup, Appl. Phys. Lett. 50, 1586 (1987).

J. Vac. Sci. Technol. A 4, 2169 (1986).
[2]G. L. Destefanis, J. Cryst. Growth 86, 700 (1987).
[3]T. M. Kao and T. W. Signon, Appl. Phys. Lett. 49, 464 (1986).
[4]G. Bahir, R. Kalish, and Y. Nemirovsky, Appl. Phys. Lett. 41, 1057 (1982).
[5]R. Kalish and G. Bahir, J. Cryst. Growth 72, 474 (1985).
[6]J. Baars, H. Sonkwind, and Ch. Fritzsche, J. Cryst. Growth 86, 762 (1987).
[7]R. Kalish, R. Fastow, V. Richter, and M. Shaanan, Appl. Phys. Lett. 51, 1158 (1987).
[8]C. Uzan-Saguy, D. Lazar, and R. Kalish, to be presented at the Fourth International Conference on II-VI Compounds, Berlin 1989 (to be published in J. Cryst. Growth).
[9]J. F. Ziegler, G. Cuomo, and J. P. Biersack, TRIM 89 Computer Code, "The Stopping and Range of Ions in Matter," 1989.
[10]G. L. Destefanis, Nucl. Instrum. Methods, 209/210, 567 (1983).
[11]J. Baars, H. Hurrle, W. Rothemund, C. R. Fritzsche, and T. Jakobus, J. Appl. Phys. 53, 146 (1982).
[12]L. O. Bubulac, J. Cryst. Growth 86, 723 (1987).

Elsevier Science Publishers B.V., P.O. Box 1991, Amsterdam
Northprint: JCG121AA 50C
Page: 5 1st proof:
IN ALL CORRESPONDENCE CONCERNING THIS PAPER REFER TO:
CRYS 121AA

Journal of Crystal Growth 00 (1989) JCG121AA
North-Holland, Amsterdam

Proceedings of the 4th International Conference on II-VI compounds Semiconductors
To be published in Journal of Crystal Growth

ELECTRICAL PROPERTIES OF $Hg_{1-x}Cd_xTe$ ($x = 0.21$) ANNEALED BY IMMERSION IN A HOT MERCURY BATH

C. UZAN-SAGUY, D. LASER *, and R. KALISH

Solid State Institute, Technion-Israel Institute of Technology, Haifa 32000, Israel

Annealing of $Hg_{1-x}Cd_xTe$ ($x = 0.21$) by immersion in a hot Hg bath has been investigated with regard to the electrical properties of as-grown and ion implanted samples. The method was found to be comparable to other more complicated annealing techniques as for improving the electrical properties of HgCdTe deduced from Hall and differential Hall effect measurements. As-recrystallized p-type samples can be converted to good n-type following immersion for 50 min the Hg bath at 260 °C. This annealing, when performed at 250 °C for just a few minutes, improves the mobility of undoped n-type samples up to 50%. Electrical activation of B implants in $Hg_{0.79}Cd_{0.21}Te$ can be achieved following immersion for 8 min in the Hg at 320 °C.

1. Introduction

The narrow band gap semiconductor $Hg_{1-x}Cd_xTe$ with the composition $x = 0.2$ is, up to date, the most widely used material for the fabrication of infrared detectors active at about 10 μm. The doping of this semiconductor is complicated by the fact that its electrical properties are determined by defects and deviations from stoichiometry and not only by electrically active impurities. Hg vacancies are active acceptors, while Hg interstitials are believed to be donors. As-grown HgCdTe crystals grown by the solid state recrystallization method are usually Hg vacancy rich and therefore present high p-type conductivities with poor mobility. Ion implantation damaged HgCdTe always exhibits n^+ conductivity with low mobility [1–3]. In both cases, whether as-grown or ion implanted, thermal treatment of HgCdTe is often needed. This, however, must be done under such conditions that avoid Hg loss and sometimes even allow indiffusion of Hg. Post-growth annealing under Hg low pressure is known to improve the mobility and reduce the acceptor concentration, while, if performed under Hg overpressure, the annealing turns the material n-type with high mobility [4]. Post-implantation annealing is usually done either under Hg pressure or on encapsulated samples to avoid Hg loss. Both these methods are complicated since they require capping (i.e. sputter deposition of ZnS or of SiO_2 or growth Hg native oxide) or annealing under special environmental conditions in closed ampoules (under excess Hg or noble gas pressure). Recently, we reported [5] on a new, very simple annealing technique, which does not require any encapsulation or ampoules, yet is carried out in a Hg rich atmosphere. In this technique, the sample, mounted in a special arrangement, is immersed for a given time in a hot Hg bath at the required temperature. In a previous publication [5], we have shown by employing ion beam probing techniques (Rutherford backscattering (RBS) and proton induced X-ray emission (PIXE)) that good near-surface crystal quality (i.e. damage removal) and stoichiometry (i.e. no Hg loss) could be achieved by this immersion annealing technique. In the present work we report on the effectiveness of the Hg bath immersion annealing with regard to the electrical properties of as-grown and ion implanted HgCdTe samples. We demonstrate by using Hall effect measurements that this method is comparable to other annealing methods as for improving the electrical properties of as-grown p-type and n-type HgCdTe. Moreover, successful electrical activation of B implants in HgCdTe is

* SCD, P.O. Box 2250, Haifa, Israel.

REQUEST
Author, please indicate
- printer's errors in BLUE
- author's changes in RED

obtained by post-implantation immersion annealing [6].

2. Experimental

The following $Hg_{1-x}Cd_xTe$ crystals with the composition $x = 0.21$ grown by the solid state recrystallization method were used: (i) as-recrystallized p-type samples (μ_p(77 K) = 150 $cm^2\ V^{-1}\ s^{-1}$ and p(77 K) = $10^{17}\ cm^{-3}$); (ii) n-type samples obtained after prolonged annealing in Hg vapor (closed ampoules at $T = 260\,^\circ C$ for $t = 1$ month, μ_n(77 K) = 70,000 $cm^2\ V^{-1}\ s^{-1}$, n(77 K) = $4 \times 10^{14}\ cm^{-3}$); (iii) doped p-type samples (μ_p(77 K) = 600 $cm^2\ V^{-1}\ s^{-1}$, p(77 K) = $6 \times 10^{15}\ cm^{-3}$). All samples were ⟨111⟩ single crystals; they were mirror-polished and etched in a solution of bromine in methanol followed by rinsing in pure methanol. The annealing apparatus, placed in a well-vented hood, is composed of a standard pyrex flask filed with pure Hg, the temperature of which is measured by a thermocouple embedded in a quartz tube (fig. 1). The annealing temperature is maintained at the desired temperature by a simple temperature controller. The sample to be immersion annealed is sandwiched between two clean Si wafers and the whole assembly is placed in a small stainless-steel box, the dimensions of which fit tightly to those of the two Si caps. A lid with a fine thread enables closing the box while gently pressing on the assembly in a way which prevents any wetting of the samples but allows the penetration of Hg vapor. The volume above the mercury surface is filled with argon to avoid Hg oxidation. The samples were immersed in the hot Hg bath for times ranging between 5 min and 50 h at temperatures varying between 200 and 356 °C (boiling point of Hg). The near surface crystallinity was evaluated by Rutherford backscattering (RBS) combined with channeling in the ⟨111⟩ direction using 320 keV protons. The electrical properties of the samples were determined by Hall effect and differential Hall effects measurements at 77 K using the Van der Pauw geometry, in a magnetic field of 2 or 6 kG.

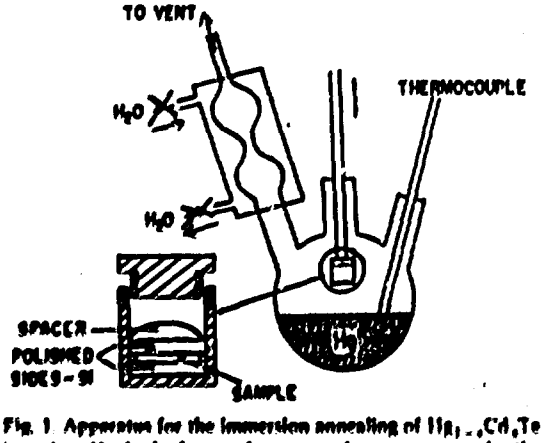

Fig. 1. Apparatus for the immersion annealing of $Hg_{1-x}Cd_xTe$ in a hot Hg bath. Insert shows sample arrangement in the stainless-steel box.

3. Results

3.1. Type conversions of as-recrystallized p-type $Hg_{0.79}Cd_{0.21}Te$

Conversion of as-recrystallized p-type samples to n-type was performed by immersion annealing for increasing times at 260 °C. This temperature was chosen as it is the temperature conventionally used when annealing is carried out in a sealed quartz ampoule with excess Hg [7]. Figs. 2a and 2b show the changes in carrier concentration and mobility as a function of immersion time. In the preliminary annealings (samples 1 and 2), the duration of the immersion was progressively increased to follow the improvement of the electrical characteristics (solid lines and dashed lines). Repeating this process too many times was found, however, to deteriorate the sample surface quality, and thus its electrical properties. The rise in apparent p-type carrier concentration and the reduction in mobility measured at a magnetic field of 6 kG in sample 1 (solid line, open circles) prior to type conversion is indicative of the buildup of a thin n-type layer on the surface. Following non-interrupted 50 h immersion in the hot Hg, the donor concentration reached $4 \times 10^{14}\ cm^{-3}$ and a mobility of $10^5\ cm^2\ V^{-1}\ s^{-1}$ at 2 kG (sample 3, solid dashed lines). The results were found to depend

FILE: 814009JAP 1 QUEUE:JAP-JAP
IS: pasteup FMT: alpxr
BY:OCR;16/02,19:19 REV:MARGA;28/02,19:27
01-MAR-90 08:18:17

814009JAP = 814009JAP

Evolution of point to extended defects in low-temperature implanted $Hg_{0.76}Cd_{0.24}Te$

V. Richter and R. Kalish
Solid State Institute, Technion-Israel Institute of Technology, Haifa 32 000, Israel

(Received 24 October 1989; accepted 15 January 1990)

The transition from point defects, frozen in at low-temperature ion implanted $Hg_{1-x}Cd_xTe$ ($x = 0.24$), to extended defects has been monitored through ion channeling experiments in the temperature range 100–360 K. It is found that the transition exhibits time and temperature dependencies characteristic for diffusion processes with exceptionally low parameters. The extended defects formed by the agglomeration of frozen-in point defects are found to roughly correspond in depth to the implant range, in contrast to defects directly created by room-temperature implantation which extend much deeper into the crystal.

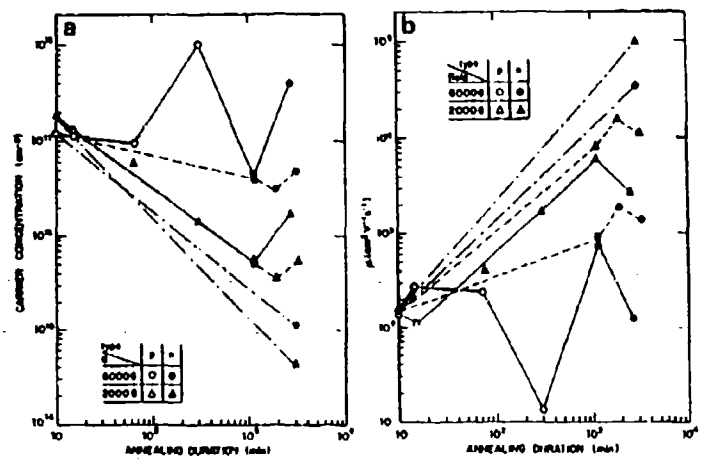

Fig. 2. Carrier concentration (a) and Hall mobility (b) of as-recrystallized p-type $Hg_{0.79}Cd_{0.21}Te$ samples immersion annealed in the Hg bath at 260 °C as function of annealing duration, p-type conductivity is represented by open symbols, while the full symbols correspond to n-type conductivity, the circles (●/○) and the triangles (▲/△) indicating Hall measurements in a magnetic field of 6000 kG or 2000 kG, respectively. Sample 1 (solid lines) and 2 (dashed lines) were annealed step by step up to 50 h while sample 3 (dashed solid lines) was annealed for 50 h in a simple step.

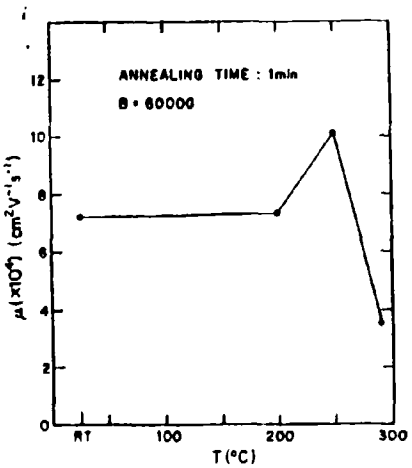

Fig. 3. Hall mobility of n-type $Hg_{0.79}Cd_{0.21}Te$ samples immersion annealed in a hot Hg bath for 1 min as a function of temperature.

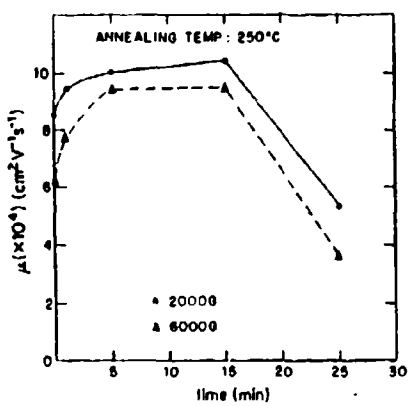

Fig. 4. Hall mobility of n-type $Hg_{0.79}Cd_{0.21}Te$ samples immersion annealed in a hot Hg bath at 250 °C as a function of time. The solid and dashed lines show the mobility obtained in a magnetic field of 2 and 6 kG, respectively.

strongly on the value of the magnetic field, possibly due to mixed conductivity [8].

3.2. Improvement of n-type $Hg_{0.79}Cd_{0.21}Te$

Several n-type $Hg_{0.79}Cd_{0.21}Te$ samples, annealed in the conventional way (under Hg pressure in an ampoule), could be improved by the present immersion annealing method. The improvements of mobility as a function of annealing temperatures for a fixed time of 1 min and as a function of annealing times for a fixed temperature of 250 °C are shown in figs. 3 and 4. As can be seen in fig. 3, the mobility improves with increasing temperature up to 250 °C, beyond which it starts to deteriorate. Fig. 4 shows that heating at 250 °C for times up to 15 min improves the mobility, but further heating damages the crystal. Under optimal conditions (250 °C for 1 min), an improvement in the mobility of nearly 50% (70,000 to 100,000 $cm^2\ V^{-1}\ s^{-1}$) was obtained; this increase in mobility was accompanied by a similar decrease in carrier concentration. Indeed, ion channeling measurements have shown that the crystallinity of the above samples exposed to Hg immersion treatment has been improved. Fig. 5 shows that annealing at 250 °C for 4 min reduces the dechanneling of the virgin spectrum

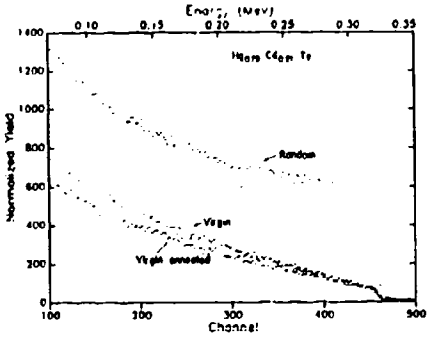

Fig. 5. Rutherford backscattering channeling spectra of 320 keV protons in the (111) direction, of virgin $Hg_{0.79}Cd_{0.21}Te$, prior to annealing (virgin) and following immersion for 4 min at 250 °C in a hot Hg (virgin and annealed).

Table 1
Mobility and carrier concentration obtained for $Hg_{0.79}Cd_{0.21}Te$: (I) B/Ne implanted samples before and after immersion annealing (320 °C, 8 min); (II) virgin sample before and after immersion annealing (320 °C, 8 min)

Sample	Implanted ion	Anneal 320 °C, 8 min	Conductivity type	Mobility ($cm^2\ V^{-1}\ s^{-1}$)	Carrier concentration (cm^{-3})
I	-	No	p	600	6×10^{15}
I	B	No	n	3000	2×10^{15} [a]
I	Ne	No	n	3000	2×10^{15} [a]
I	B	Yes	n	28000 [b]	1×10^{17} [a]
I	Ne	Yes	p	70	2×10^{16}
II	-	No	p	450	1×10^{16}
II	-	Yes	p	200	4×10^{16}

[a] Deduced for a thickness of 1 μm.
[b] This mobility was measured at a depth of 1.2 μm. Prior to any etching the measured mobility was 20,000 $cm^2\ V^{-1}\ s^{-1}$.

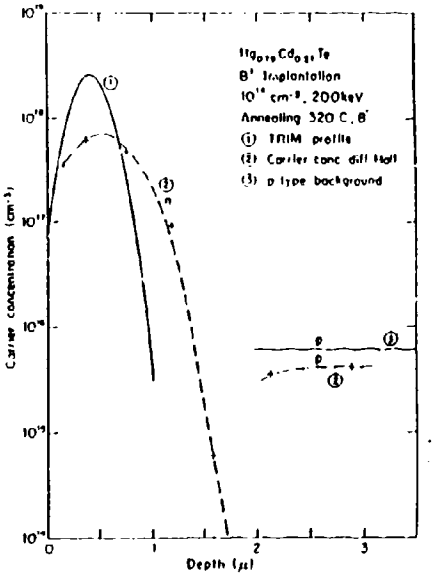

Fig. 6. Electrical conductivity profile as deduced from differential Hall measurements on $Hg_{0.79}Cd_{0.21}Te$ implanted with B (10^{14} cm^{-2}; 320 keV) and immersion annealing for 8 min at 320 °C. The calculated profile of as-implanted B is shown for comparison.

indicating that some defects have been removed by the further immersion annealing.

3.3. Electrical activation of B implanted $Hg_{0.79}Cd_{0.21}Te$

Two halves of a p-type doped $Hg_{0.79}Cd_{0.21}Te$ wafer (sample I) have been implanted at room temperature, one with 200 keV B to a dose of 10^{14} cm^{-2} and the other with 320 keV Ne to a dose of 3×10^{13} cm^{-2}. The dose and energy for the Ne implantation have been chosen such that the amount of damage and its profile coincide with those caused by the B implantation. The two implanted samples have been immersion annealed for 8 min at 320°C, together with a control sample, cut from the same ingot (sample II), which has not been implanted. The electrical properties of the unimplanted, implanted and annealed samples have been determined from Hall measurements in a magnetic field of 2 kG. While prior to the annealing, the B and Ne samples exhibit identical n-type conductivities, attributed to radiation damage, their properties are drastically different following the annealing. As shown in table 1, the donor carrier concentration of the B implanted and annealed sample has been strongly reduced while its mobility has been increased by one order of magnitude. The Ne implanted sample, on the other hand, has returned p-type as a result of the immersion annealing. The poor mobility and high carrier concentration exhibited by this sample may be indicative of mixed conductivity, possibly caused by donor activity due to some residual not completely annealed damage. In contrast to the implanted samples, the annealed virgin sample has remained p-type showing that no significant indiffusion of Hg has happened during the annealing process.

Differential Hall measurements performed on the B implanted and annealed sample have shown that the carrier concentration peaks at a depth of 5000 Å, the junction being located about 1.5 μm below the surface. As seen in fig. 6, the electrical profile is deeper than the implant profile deduced from range calculations. Since it is known that B does not substantially diffuse in HgCdTe at temperatures and times relevant to the present experiment [9,10], we concluded that the deep donor activities can be attributed to B related complexes and possibly to a channeling tail which extend deeper into the crystal than the calculated B profile [11].

4. Conclusion

We have shown that the newly developed immersion annealing technique is comparable to other annealing methods as for improving the electrical properties of HgCdTe. The near surface conductivity of as-recrystallized p-type samples can be converted by this method to n-type with a low carrier concentration and a high mobility. The mobility of n-type samples can be increased following immersion annealing in a hot Hg bath and boron implants can be electrically activated by this simple annealing technique.

Acknowledgement

This research has been supported in part by the US Army (contract No. DAJA 45-86-C-0011).

References

[1] L.O. Bubulac, W.E. Tennant, R.A. Riedel and T.J. Magee, J. Vacuum Sci. Technol. 21 (1982) 251.
[2] L.O. Bubulac, W.E. Tennant, D.S. Lo, D.D. Edwall, J.C. Robinson, J.S. Chen and O. Bostrup, J. Vacuum Sci. Technol. A5 (1987) 3166.
[3] S. Margalit, Y. Nemirovsky and I. Rolstein, J. Appl. Phys. 50 (1979) 6386.
[4] C.L. Jones, M.J.T. Quelch, P. Capper and J.J. Gosney, J. Appl. Phys. 53 (1982) 9080.
[5] R. Kalish, R. Fastow, V. Richter and M. Shaanan, Appl. Phys. Letters 51 (1987) 1158.
[6] C. Uzan-Saguy and R. Kalish, Appl. Phys. Letters, in press 55 (1989) 1091.
[7] A.J. Syllaios and M.J. Williams, J. Vacuum Sci. Technol. 21 (1982) 201.
[8] A. Smith, Semiconductors (Cambridge University Press, Cambridge, 1978) ch. 5, p. 114.
[9] G.L. Destéfanis, Nucl. Inst. Methods 209/210 (1983) 567.
[10] J. Baars, H. Hurrle, W. Rothemund, C.R. Fritzsche and T. Jakobus, J. Appl. Phys. 53 (1982) 146.
[11] L.O. Bubulac, J. Crystal Growth 86 (1987) 723.

Ion implantation induced damage in low-x $Hg_{1-x}Cd_xTe$ is of technological importance since the damage in that material is an electrically active donor; a fact which is utilized in the realization of infrared detectors in $Hg_{1-x}Cd_xTe$ by producing n(damage)-on-p devices by ion implantation. The understanding of the nature and thermal stability of this damage is therefore of great technological importance and of much scientific interest. Previous studies[1] on how HgCdTe damages by room-temperature ion implantation have shown that only extended defects, most likely dislocations, are present in the implanted material and that the damage, when induced by heavy ions, reaches depths which much exceed the projected range of the implants. Computer simulations of the damage cascades in HgCdTe, which do not take into account defect diffusion and agglomeration, obviously predict only the presence of point defects with a distribution which roughly coincides with that of the implant. The transition from frozen-in point defects to extended defects, which certainly takes place at some annealing stage and which must be associated with the diffusion of point defects in HgCdTe (most likely Hg vacancies and interstitials) has never been observed. In the present work we report on the observation of this transition and deduce the diffusion parameters which can be associated with it. Furthermore, we find that the profile of the extended defects caused by low-temperature implantations followed by annealing to room temperature is substantially shallower than that observed for room-temperature implantations; a fact which may be of importance in the realization of shallow n(damage)-on-p photodiodes.

Rutherford backscattering (RBS) channeling measurements[2] carried out at different temperatures on low-temperature implanted HgCdTe are used in the present work to learn about the depth and the nature of the damage in implanted and gradually annealed samples. The crystals used were (111)-oriented $Hg_{1-x}Cd_xTe$ ($x \approx 0.24$). They were mounted on a triple-axis goniometer with provision to cool and heat the specimen between 100 and 400 K. Indium ions were implanted into randomly oriented crystals held at 100 K at an energy of 320 keV to a dose of 2×10^{13} cm^{-2}. Such an implantation is sufficient to create a substantial number of extended defects in that material when performed at room temperature.[1] RBS channeling measurements with 320keV protons were carried out on the cold sample immediately following the implantation [see Fig. 1(a)]. Different experiments were carried out to study the transformations that these defects undergo with temperature. (i) A cold implanted sample was allowed to warm to room temperature at a roughly constant rate of about 1 K/min and RBS channeling spectra were taken at different times during the warm-up period. Representative spectra are shown in Fig. 1(b) and 2(c). (ii) The sample was further heated to 360 K and was kept at this temperature for 5 h [Fig. 1(d)]. (iii) Samples implanted at 100 K were heated to 167, 191, and 218 K at which temperatures they were kept and RBS channeling spectra were taken at different times observing the isothermal evolution of the defects. The following observations are directly evident (Fig. 1): Following the implantation at 100

2

([spectrum of Fig. 1(a)] the channeling RBS spectrum eaches the random level, indicating that the material has urned amorphous to a dep h of about 1000 Å which coin- ides well with the calculated range[3] of the In implants in $Ig_{0.76}Cd_{0.24}Te$ ($R_p \simeq 700$ Å, $\Delta R_p \simeq 300$ Å). The mea- ured $\chi_{min} = 82\%$ value (i.e., the ratio between the chan- eled and the random spectra) just behind the damage peak an be fully accounted for by the dechanneling caused by the morphous layer.[4] Upon the warming up of the sample a hrinkage of the damage peak without substantial reduction n peak height can be noticed. Interestingly, the narrowing of he damage peak is not accompanied by a reduction in χ_{min} ehind the damage peak, as would be expected if its origin as only in the amorphous layer. Hence other new defects hich give rise to this dechanneling must have been formed uring the shrinkage of the point-defect-rich region. This is ost pronounced in the spectrum of Fig. 1(c) (243 K), in hich no damage peak can be seen any more, yet the dechan- eling level remains unchanged. Further heating ($T = 360$) [Fig. 1(d)] partially transforms the RBS channeling pectrum to that commonly observed for RT implanted IgCdTe [Fig. 1(e)], exhibiting a rise in dechanneling hich becomes more gradual at a well-defined depth. It has een shown[1] that such a spectrum is typical for a layer rich in tended defects, and that the energy in the backscattered pectrum at which the break (knee) occurs roughly corre- ponds to the thickness of the damaged layer. The depth of he knee in the present experiment, in which the sample has een implanted at a low temperature and has later been al- owed to warm up, is substantially shallower than that ob- rved after identical room-temperature implantations [Fig. (e)].

Quantitative information on the shrinkage of the dam- e peak Δz at different temperatures or times was deduced om the RBS spectra by fitting the relevant parts to 4° or 6° olynomials. This enabled the analytical determination of he inflection points in the spectra thus offering a systematic easure for the changes in damage peak width. Three differ- nt modes of essentially the same analysis (different degrees f the polynomial and different programs) have been em- loyed yielding roughly the same results. The shrinkage Δz educed in that way for the case of the isothermal annealing 191 K is plotted against $\sqrt{t}$ (t being the annealing time) in g. 2. The three sets of points are the result of the different odes of analysis; their scatter is an indication for their un- rtainty. A straight line can reasonably well be fitted hrough the points yielding a diffusion coefficient $D(191$) $= (1.1 \pm 0.1) \times 10^{-16}$ cm²/s.

The data taken at 167 and 218 K were analyzed in a milar way yielding diffusion coefficients $D(167$ K) $(0.2 \pm 0.1) \times 10^{-16}$ cm²/s and $D(218$ K) $(9 \pm 2) \times 10^{-16}$ cm²/s. An Arrhenius plot of these data is shown in Fig. 3 yielding $D = (4.2 \times 10^{-10}) \exp[-(0.25 \pm 0.03)/kT]$.

The analysis of the second kind of experiment, in which the shrinkage of the damage peak has been observed during the nonisothermal warming up of the sample, is less straightforward, hence no accurate values for the diffusion parameters were deduced. Nevertheless, a rough analysis shows that these data also support a very low activation energy ($E_a = 0.12$ eV) and a small pre-exponential factor ($D_0 = 8 \times 10^{-15}$ cm²/s).

The transformation from point to extended defects in implantation-damaged HgCdTe observed here at low temperatures should be related to some species, possibly Hg interstitials,[5] diffusing in the disordered crystal to agglomerate and form extended defects, most likely dislocation loops. Indeed the results exhibit time and temperature dependencies characteristic for diffusion processes, the diffusion parameters extracted from the present results are, however, abnormally low. The diffusion in crystalline II-VI materials have recently been reviewed by Shaw,[6] who has also compiled a large number of experimental data for self and impurity diffusion in HgCdTe ($x = 0.2$). Despite the large discrepancies which exist between results reported by different groups Shaw shows that most data follow a linear relationship given by $\ln D_0 = 15.0 E_a - 23.7$.

The present results may actually not be comparable with data on diffusion in HgCdTe since the latter deal with a different temperature regime (usually 400–700 K) and are for diffusion in nondamaged crystals. Nevertheless, the values for D_0 and E_a found here fit Shaw's relationship rather well. The fact that the activation energy determined here is substantially lower than that measured by others (0.5 eV $< E_a < 1.5$ eV) is not surprising since the diffusion of the point defects of the present experiment is in a damaged, vacancy-rich crystal. Furthermore, the diffusion of atoms to extended defects already existing in the crystal to enable their further growth may be driven by strain fields, which will also result in an apparent lowering of the activation energy. The abnormally low values for D_0 and E_a measured here for low temperatures in highly disordered HgCdTe can quantitatively be explained by employing the short-lived large energy fluctuation kinetic model proposed by Khait.[7] A detailed analysis of the results in light of that model will be given elsewhere.[8]

This work has been supported in part by the U.S. Army (Contract No. DAJA45-86-C-Od). The help of C. Uzan-Saguy, D. Comedi, and N. Moriya at various stages of the experiments and analysis is acknowledged.

[1] C. Uzan-Saguy, D. Comedi, V. Richter, R. Kalish, and R. Triboulet, J. Vac. Sci. Technol. A 7, 2575 (1989).

[1]W. K. Chu, J. W. Mayer, and M. A. Nicolet, *Backscattering Spectrometry* (Academic, New York, 1978).
[2]J. F. Ziegler, J. P. Biersack, and G. Cuomo, TRIM'85 program, version 5.0 (Transport of Ions in Matter).
[3]L. Meyer, Phys. Status Solidi B 44, 253 (1971).
[4]Y. Kim, A. Ourmazd, M. Bode, and R. D. Feldman, Phys. Rev. Lett. 63, 636 (1989).
[5]D. Shaw, J. Cryst. Growth 86, 778 (1988).
[6]Yu. L. Khait, Phys. Rep. 99, 237 (1983).
[7]Yu. L. Khait and V. Richter (unpublished).

FIG. 1. RBS channeling spectra of 320 keV protons of In-implanted (320 keV 2×10^{13} cm^{-2}) HgCdTe taken at different temperatures: (a) as-implanted (T = 100 K), (b) 223 K, (c) 243 K, (d) 5 h at 360 K, and (e) following room-temperature implantation. Random and channeled spectra of the virgin crystal are also shown.

FIG. 2. The time dependence of the shrinkage (z) of the amorphous layer in 100 K implanted HgCdTe held at a constant temperature of 191 K. The three sets of data points represent three different modes of analysis.

FIG. 3. Arrhenius plot of the diffusion coefficients governing damage evolution in cold-implanted HgCdTe obtained at three constant temperatures: 167, 191, and 218 K.

Buildup of ion implantation damage in $Hg_{1-x}Cd_xTe$ for various x values

C. Uzan-Saguy, D. Comedi, V. Richter, and R. Kalish
Solid State Institute, Technion-Israel Institute of Technology, Haifa 32000, Israel

R. Triboulet
Laboratoire de Physique des Solides, Centre National de la Recherche Scientifique, 1 Place A. Briand, 92195 Meudon Principal Cedex, France

(Received 28 October 1988; accepted 4 March 1989)

The buildup of damage induced by In ion implantation into $Hg_{1-x}Cd_xTe$ for various composition ($x = 0$, $x = 0.24$, $x = 0.4$, $x = 0.7$, and $x = 1$) was measured by means of channeling Rutherford backscattering spectroscopy (RBS). Damage profiles were extracted from the spectra using a model based on Quéré's dechanneling treatment. Despite the large difference in bond nature and the related physical properties between the different compositions, the general trends in damage formation were found similar for all x values studied, though displaced by about two orders of magnitude in dose, HgTe damaging much easier than CdTe. For all compositions, different types of damage seem to be created at different stages during the implantation. The results can be understood if agglomeration of point defects to extended defects followed by a redistribution of the defects to deeper lying clusters with increasing dose is assumed.

I. INTRODUCTION

Among the ternary II-VI compound semiconductors, $Hg_{1-x}Cd_xTe$ (MCT) is possibly the most widely studied. The fact that $Hg_{1-x}Cd_xTe$ is a mixed crystal containing a fraction x of CdTe, a semiconductor with a fairly wide band gap of 1.6 eV, and $(1-x)$ of HgTe, a semimetal with a negative gap of -0.3 eV makes it possible to tailor the material by adjusting x to any desired band gap between 0 and 1.6 eV.[1] The compositions of MCT around $x = 0.2$ and $x = 0.3$ have found wide use as infrared detectors since they have band gaps which cover the two atmospheric windows for IR radiation at 8 to 12 and 3 to 5 μm, respectively. Recently interest in MCT with $x = 0.7$ has arisen due to the cutoff wavelength of this material which corresponds well with that required for minimum attenuation in optical fibers (1.3 μm).[2] Pure CdTe ($x = 1$) has been used for the detection of visible light or gamma radiation.[3]

The electrical properties of $Hg_{1-x}Cd_xTe$ are determined by composition (x), by deviation from stoichiometry, by native defects, and by the presence of impurities. In particular, n-type conductivity has been realized in low x MCT ($x = 0.2$ to 0.3) by ion implantation.[4,5] Even though the implant most commonly used for that purpose is B (a potential donor in MCT), implantation of any other ion also results in n-type conductivity, indicating that the electrical properties are governed by the implantation-induced damage, rather than by impurity doping.[6-9] Interestingly, the doping effects that the implantation causes extend much deeper into the crystal than the range of the primary implants, showing that the damage-related donor states cannot be directly associated with simple point defects. The effects of ion damage on higher x MCT has been studied to a much lesser extent. However, it has been shown most recently that the implantations of Ar, In, or Xe into p-$Hg_{0.7}Cd_{0.3}Te$ ($x = 0.7$) turns the material highly resistive.[10]

The study of the nature of implantation-induced damage in $Hg_{1-x}Cd_xTe$ for various values of x is of importance because of the use made of the damage itself as a doping mechanism. It is, however, also of basic interest due to the gradual, yet rather extreme, changes that the material undergoes with x. Both HgTe and CdTe are rather soft materials because of their large bond length ($d_{CdTe} = 2.804$ Å; $d_{HgTe} = 2.797$ Å) and polarity (ionic coefficient F_i) which is greater in CdTe ($F_i = 0.71$) than in HgTe ($F_i = 0.65$). Nevertheless the HgTe bond, mostly metallic, is considerably weaker than the CdTe bond ($E_{HgTe} = 0.58$ eV; $E_{CdTe} = 0.89$ eV); hence the enhanced tendency of the Hg rich alloys to lose Hg.[11-13]

The question of how the various alloys of MCT respond to implantation damage is the subject of the present work, in which a systematic study of the buildup of damage in $Hg_{1-x}Cd_xTe$ with compositions $x = 0$, 0.24, 0.4, 0.7, and 1 as a result of increasing dose of indium ion implants has been carried out. While, as expected, it was found that Hg rich (low x) crystals damage much easier than those with higher x composition, some features, common to all alloys could be extracted from the data so that general insight into the damage mechanism in MCT could be obtained.

II. EXPERIMENTAL

$Hg_{1-x}Cd_xTe$ crystals with compositions $x = 0$ (pure HgTe), 0.24, 0.4, and 0.7 were grown by the traveling heater method.[14] Pure CdTe ($x = 1$) was grown by the modified Bridgman technique.[15] Samples, 15 mm in diameter oriented with the <111> axis perpendicular to the surface, were cut out of the ingots, mirror polished, and etched in a solution of bromine in methanol followed by proper rinsing in methanol. The specimens were mounted on a three-axis goniometer and were subjected to consecutive Rutherford backscattering/channeling measurements and indium ion implantation at ever increasing doses. The channeling experiments were carried out with 320 keV protons collimated through 1 mm apertures with an angular spread $<0.04°$ backscattered into a detector set at 165°. To perform the implantations, the beam apertures were opened to 0.5×1 cm^2, the crystal was rotated to a random direction, and the particle detector was shielded from backscattered heavy

 0734-2101/89/042678-05$01.00

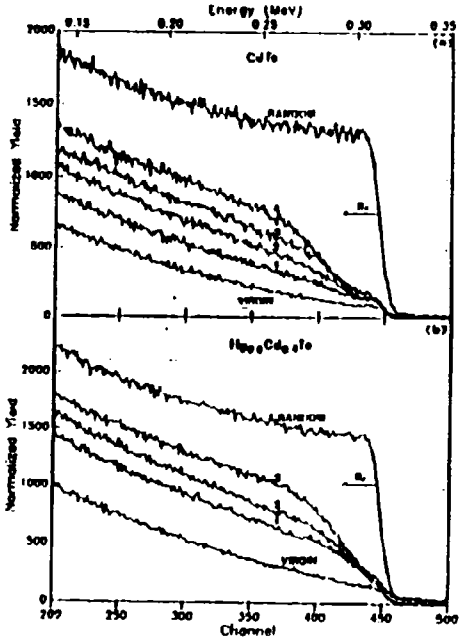

FIG. 1. Channeling Rutherford backscattering spectra obtained for (a) pure CdTe and (b) $Hg_{0.8}Cd_{0.2}Te$ implanted with 320 keV In ions. In (a), spectra 1, 2, 3, and 4 correspond to implantation doses of 10^{14}, 2×10^{14}, 4×10^{14}, and 2×10^{15} cm^{-2}, respectively, while in (b), spectra 1, 2, and 3 correspond to doses of 10^{13}, 4×10^{13}, and 2×10^{14} cm^{-2}, respectively.

ions. ^{115}In ions, extracted from the same ion source as used for the RBS experiments, were accelerated to 320 keV and were homogeneously swept across the specimen. All implantations were carried out at room temperature into heat-sunk samples, keeping the beam current areal density constant at 40 nA/cm^2. Under such conditions negligible beam-induced heating of the sample is expected. In order to minimize damage caused by the probing beam, proton currents of <3 nA were used. The buildup of damage, as function of In implantation dose was measured for each of the compositions studied. All measurements were performed twice in completely independent runs and yielded consistent results.

III. RESULTS

In the present experiment, use was made of medium energy proton backscattering to assess the damage in implanted MCT. The fact that fairly low energy protons were used assured that there was practically no energy discrimination between protons backscattered from Hg, Cd, or Te atoms (the difference in the most extreme backscattered energies being of the order of the detector resolution). The results obtained here, therefore, present the behavior of the MCT crystal as a whole. High-energy, heavy ion backscattering[16] or PIXE channeling experiments[17] are needed to obtain more detailed information on the behavior of the separate constituents of the crystals studied. Despite the fact that rather substantial differences in bond properties exist between the extreme cases studied here ($x=0$ to 1), the present results show that, nevertheless, many features are common to all compositions.

Figure 1 shows representative channeling RBS spectra obtained for pure CdTe [Fig. 1(a)] and for $Hg_{0.8}Cd_{0.2}Te$ [Fig. 1(b)] implanted with In ions. The spectra obtained for the other compositions studied look rather similar. For CdTe, the doses at which substantial changes in the damage occur vary between 10^{14} cm^{-2} and 2×10^{15} cm^{-2} and for $Hg_{0.8}Cd_{0.2}Te$ between 10^{13} cm^{-2} and 2×10^{14} cm^{-2}. The following features, common to all compositions studied, can be noticed already from the raw data: (i) The damage always reveals itself through a gradual dechanneling of the probing protons. This dechanneling is reflected in a constant rise in the backscattering yield with increasing depth. Such a behavior is usually observed for metals implanted at room temperature, and is caused by extended defects. At a well-defined depth, which is substantially larger than the projected range of the implants (800 Å), a change in slope ("knee") sets in. (ii) There exists a near saturation of damage, i.e., above a certain implantation dose the increment of damage with dose, as seen in the RBS spectra, is small. (iii)

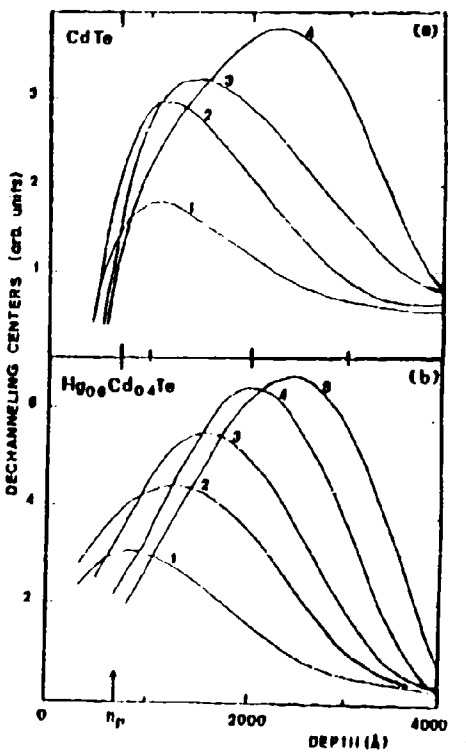

FIG. 2. Damage depth profiles extracted from the RBS channeling data presented in Figs. 1(a) (CdTe) and 1(b) ($Hg_{0.8}Cd_{0.2}Te$). In Fig. 2(a) the curves 1, 2, 3, and 4, correspond to implantation doses of 2×10^{14}, 4×10^{14}, 8×10^{14}, and 2×10^{15} cm^{-2}, respectively. In Fig. 2(b), the curves 1, 2, 3, 4, and 5 represent the damage profile obtained following implantation at doses of 4×10^{13}, 8×10^{13}, 2×10^{14}, 4×10^{14}, and 8×10^{14} cm^{-2}, respectively.

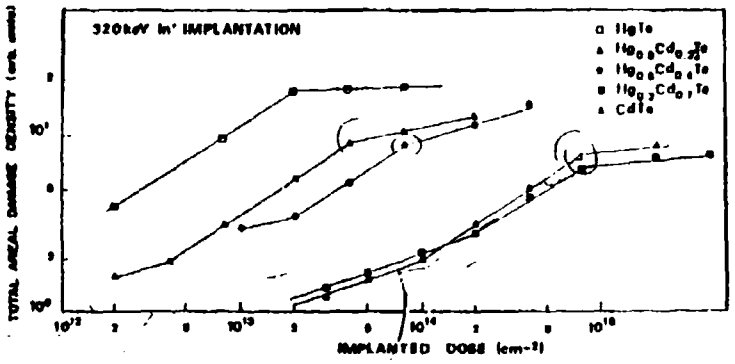

FIG. 3. Total areal damage (arbitrary units) as function of In ion implantation dose for the different alloy composition $x = 0$, $x = 0.24$, $x = 0.4$, $x = 0.7$, and $x = 1$.

The maximum dechanneling never reaches the random level, but it changes with x; the lower the x value the higher the saturation dechanneling. (iv) The minimum doses for which damage starts to be noticeable in the RBS spectra depends strongly on x. While for $x = 0.4$ [Fig. 1(b)] deviations from the virgin spectrum can be seen already for 5×10^{11} In/cm^2, noticeable damage sets in for CdTe [Fig. 1(a)] only at a dose of 10^{14} In/cm^2.

Damage profiles were extracted from the RBS channeling spectra according to the procedure proposed by Feldman,[18] Pronko,[19] Piercaux,[20] and Quéré.[21] In this approach one extracts the damage profile $N_D(z)$ as function of depth into the crystal z from the expression:

$$N_D(z) = \frac{1}{\sigma_D} \frac{d}{dz}\left\{\ln\left(\frac{\chi_D(z) - \chi_V(z)}{1 - \chi_V(z)}\right)\right\}^{-1}. \qquad (1)$$

Here $\chi_V(z)$ and $\chi_D(z)$ are the measured normalized yields for the unimplanted (virgin) and implanted (damaged) crystal evaluated at depth z. σ_D is the defect scattering cross section. In calculating the depth scales for crystals having different degrees of damage, the changes in proton stopping power with the amount of channeling which they undergo was taken into account using an iterative procedure as described by Kao.[22] For the evaluation of Eq. (1) from the experimental data, the relevant parts of the spectra (from channel 290 to channel 440) were fitted by polynomials of degrees varying between 3 and 6 depending on the shape of each experimental spectrum. With those, it was possible to analytically evaluate Eq. (1), thus yielding the depth profile of the damage. Figures 2(a) and 2(b) show the profiles extracted from the data of Figs. 1(a) (CdTe) and 1(b) ($Hg_{0.6}Cd_{0.4}Te$), respectively. The two major features evident from Figs. 2(a) and 2(b) are that the damage does not increase at a constant rate with increasing In implantation dose, and that the depth at which the damage reaches its maximum increases with increasing dose, and for the higher doses, is substantially deeper than the projected range of the implants. Figure 3 shows the integrated total damage as a function of the implantation dose for all compositions studied. It illustrates that striking similarities exist between all compositions studied with regard to the way the damage builds up with increasing implantation dose. All five lines which connect the data points in Fig. 3 exhibit a similar trend, even though they may be displaced along the dose axis by more than two orders of magnitude. Three regions can be observed in the damage versus dose curves, in particular when damage is plotted on linear axis: First a slow rise in damage with increasing dose (region I), followed by a much steeper rise (region II) which leads, at even higher doses, to a rather flat region (region III), indicating that some saturation in the damage sets in. For HgTe, region I was not observed probably because it appears at doses lower than 10^{13} cm^{-2}. Even though the transition between the three mentioned regions is not very well defined, it is possible to read from the curves of Fig. 3 the approximate doses at which the slopes of the curves change. The integrated total damage at which the "kinks" in the lines appear, are displayed in Fig. 4, as a function of x, for both the first (transition between regions I and II) and the second (transitions between regions II and III) knees in the damage versus dose curves. Interestingly, both kinks appear, for all compositions studied, after a certain threshold amount of damage, approximately common to all composition, has been created in the crystals. This may indicate that basic changes in damage properties occur when a particular density of defects, common to all alloys of MCT, is reached.

Further support for the existance of particular damage

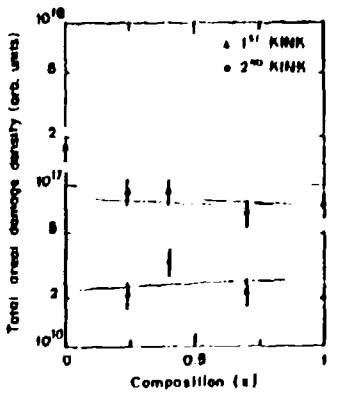

FIG. 4. Total areal damage (arbitrary units) at which the first and second kinks appeared in Fig. 3 vs alloy composition.

mon to all compositions (first kink) above which a faster growth of extended defects with increasing dose sets in (region II). This high rate damage production continues until the damages density nearly saturates (second kink) to a value which is about five times higher than for the first kink. Further ion implantation presumably breaks up the already existing extended defects releasing point defects which migrate into the crystal to form new extended defects at greater depths. The redistribution of the extended defects explains the saturation of the total damage with increasing dose and the enhanced motion of the damage maxima into the crystal in region III. The fact that the damage density integrated over the in range reduces with the square root of the dose suggests that the mechanism responsible for the defect redistribution is related to some ion assisted diffusion process.

It is evident from the present observations that the Hg rich crystals(low x) damage more and easier than those with higher x. This result is expected and is in full agreement with the fact that the Hg–Te bond is much weaker than the Cd–Te bond and that the formation energy of a metal vacancy, as calculated by Bailly,[23] is much lower for HgTe than for CdTe. However, in the case of $Hg_{1-x}Cd_xTe$ with $x = 0.7$, the damage production was found to be similar and even somewhat lower than in pure CdTe($x = 1$). This peculiar behavior cannot be explained by only bond strength considerations, but it may be connected with the fact that the microhardness of the $Hg_{1-x}Cd_xTe$ alloys exhibits a maximum around $x = 0.7$. Since microhardness is determined by the density of dislocations the higher stability of the $x = 0.7$ lattice and the lower defect production at this composition[24] may well be related.

The buildup and the reconstruction of the damage induced by In ion implantation in various x $Hg_{1-x}Cd_xTe$, was studied in the present work by Rutherford backscattering spectrometry, and has been related to the nature of the bonds and to some mechanical properties of the alloy. However, only cross sectional TEM experiments on samples of different compositions implanted at doses corresponding to the three distinct regions (Fig. 3) can confirm the explanation offered in the present work.

ACKNOWLEDGMENTS

This work was supported by the U.S. Army (Contract No. DAJA45-86-C-001). The authors thank Dr. A. Muranevitch who has kindly furnished part of the samples.

[1] R. K. Willardson and A. C. Beer, *Semiconductors and Semimetals* (Academic, New York, 1981), Vol. 18.
[2] M. Roger, T. Brossat, P. Fragnon, J. Meslage, O. Pichard, and T. Nguyen Duy, Ann. Telecommun. 38, 62 (1983).
[3] P. Siffert, Rev. Phys. Appl. 12, 105 (1977).
[4] L. O. Bubulac, W. E. Tennant, S. H. Shin, C. C. Wang, M. Lanir, E. R. Gertner, and E. D. Marshall, Jpn. J. Appl. Phys. 19, 495 (1980).
[5] G. L. Destefanis, Nucl. Instrum. Methods 209/210, 567 (1983).
[6] S. Margalit, Y. Nemirovsky, and I. Rotstein, J. Appl. Phys. 50, 6386 (1979).
[7] J. Baars, A. Hurrle, W. Rothemund, C.R. Fritzsche, and T. Jakobus, J. Appl. Phys. 53, 1461 (1982).
[8] G. L. Destefanis, J. Vac. Sci. Technol. A 3,171 (1985).
[9] J. K. Vasilyanov, S. P. Kruvyrev, and A. V. Spitsyn, Sov. Phys. Semicond. 16, 626 (1982).
[10] C. Uzan, Y. Marfaing, R. Legros, R. Kalish, and V. Richter, J. Cryst. Growth 86, 744 (1988).
[11] A. Sher, A. B. Chen, W. E. Spicer and C. K. Shih, J. Vac. Sci. Technol. A 3, 105 (1985).
[12] A. B. Chen, A. Sher, and W. E. Spicer, J. Vac. Sci. Technol. A 1, 1674 (1983).
[13] J. C. Phillips, *Bonds and Bands in Semiconductors* (Academic, New York, 1973).
[14] R. Triboulet, T. Nguyen Duy, and A. Durand, J. Vac. Sci. Technol. A 3, 95 (1985).
[15] N. R. Kyle, J. Electrochem. Soc. 118, 1790 (1971).
[16] K. Takita, T. Ipposhi, K. Murakami, K. Masuda, H. Kudo, and O. Seki, Appl. Phys. Lett. 48, 852 (1986).
[17] G. Bahir and R. Kalish, J. Appl. Phys. 54, 3129 (1983).
[18] L. C. Feldman and J. C. Rodgers, J. Appl. Phys. 41, 3776 (1970).
[19] P. P. Pronko, Nucl. Instrum. Methods 132, 249 (1976).
[20] S. U. Campisano, E. Rimini, G. Foti, and G. U. Campisano, Phys. Rev. B 18, 2078 (1978).
[21] Y. Quéré, J. Nucl. Mater. 53, 262 (1974); Radiat. Eff. 28, 253 (1976).
[22] J. M. Kao, Ph.D. thesis, Stanford University, 1987.
[23] F. Bailly, in *Proceedings of Lattice Defects in Semiconductors*, edited by R. R. Hasiguti (University of Tokyo, Tokyo and Pennsylvania State University, Pennsylvania, 1968).
[24] S. Cole, M. Brown, and A. F. W. Willoughby, J. Mater. Sci. 17, 2061 (1982).

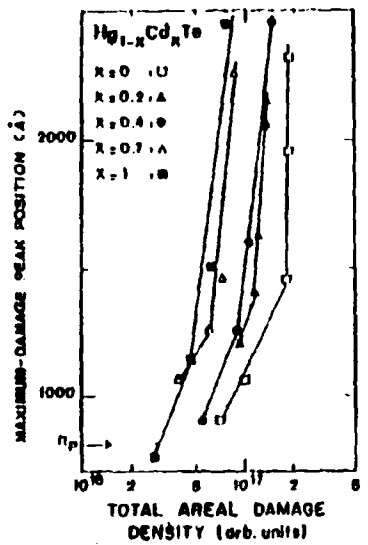

FIG. 5. Depth at which the damage reaches its maximum value vs total areal damage density (arbitrary units) for the various x studied.

levels at which distinct changes in the nature of the damage set in can be found in Fig. 5, in which the damage peak position is plotted against the total damage for all crystals studied. While for low implantation doses (i.e., low total damage levels) the damage profiles roughly peak at the projected range of the In implants, the whole damage distribution is gradually shifted inwards with increasing ion dose. This process continues until, at a particular amount of accumulated damage, which is roughly the same as that where the second kink appears (Fig. 4), the damage maxima start to move rather rapidly into the crystal. This occurs, however, without any significant increase in the total integrated damage. In other words, when this process sets in, further implantation hardly adds to the total damage, but rather it pushes the damage deeper into the crystal. Hence, above this "damage threshold," the total damage in the near surface region where the implants come to rest, is actually decreasing. By integrating the area under the damage curves over a depth bin which covers the expected implant distribution (500–1000 Å), a decrease in damage with increasing dose is indeed observed. This damage reduction is approximately inversely proportional to the square root of the dose, the proportionality factor decreasing with increasing x, as shown in Fig. 6. This suggests that some beam-induced damage redistribution sets in for all MCT compositions when a particular damage level is reached. This process is most pronounced for HgTe (highest slope of line in Fig. 6) and least for CdTe; in accord with the results on the buildup of the damage at the lower doses, which too is strongest for the low x compositions of $Hg_{1-x}Cd_xTe$.

IV. DISCUSSION

The main observations common for all x following room temperature In implantation, are summarized below.

(i) All defects observable by RBS are extended defects (most likely dislocation loops[27]). Even at high implantation doses, no lattice amorphization is reached.

(ii) The damage formation with increasing dose exhibits three regions.

(iii) The turnover doses between these regions (kinks) occur for all x at about the same total accumulated damage.

(iv) The turnover between regions II and III (second kink) is accompanied by an enhanced motion of the damage maxima into the crystal.

(v) In region III, where the total damage reaches saturation, the integrated damage around the implant range actually reduces with approximatively a square-root dependence on dose.

(vi) All the above observations seem to scale roughly monotonically with x, except for $Hg_{0.3}Cd_{0.7}Te$ ($x = 0.7$) the damage behavior of which much resembles that of pure CdTe ($x = 1$).

A possible mechanism explaining the above results is described below. At low implanted doses (region I), the point defects created by In ions migrate and agglomerate to form extended defects. These processes are enhanced in the lower x-composition of $Hg_{1-x}Cd_xTe$ because of the ionic forces existing in the lattice. As a matter of fact, the dominant ionic character of the bonds (common to all II–VI compounds) is also responsible for important defect recombination, hence, even for large implantation doses, no amorphization of the crystal is achievable at room temperature. At higher doses, the density of extended defects reaches a critical value com-

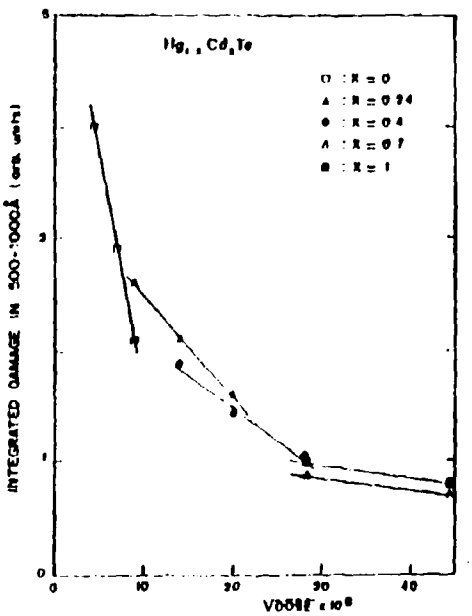

FIG. 6. Relative damage at expected implant range (integrated area over a depth bin varying between 500 and 1000 Å) vs square root of the implantation dose for all compositions studied.

mon to all compositions (first kink) above which a faster growth of extended defects with increasing dose sets in (region II). This high rate damage production continues until the damages density nearly saturates (second kink) to a value which is about five times higher than for the first kink. Further ion implantation presumably breaks up the already existing extended defects releasing point defects which migrate into the crystal to form new extended defects at greater depths. The redistribution of the extended defects explains the saturation of the total damage with increasing dose and the enhanced motion of the damage maxima into the crystal in region III. The fact that the damage density integrated over the In range reduces with the square root of the dose suggests that the mechanism responsible for the defect redistribution is related to some ion assisted diffusion process.

It is evident from the present observations that the Hg rich crystals(low x) damage more and easier than those with higher x. This result is expected and is in full agreement with the fact that the Hg–Te bond is much weaker than the Cd–Te bond and that the formation energy of a metal vacancy, as calculated by Bailly,[31] is much lower for HgTe than for CdTe. However, in the case of $Hg_{1-x}Cd_xTe$ with $x = 0.7$, the damage production was found to be similar and even somewhat lower than in pure CdTe($x = 1$). This peculiar behavior cannot be explained by only bond strength considerations, but it may be connected with the fact that the microhardness of the $Hg_{1-x}Cd_xTe$ alloys exhibits a maximum around $x = 0.7$. Since microhardness is determined by the density of dislocations the higher stability of the $x = 0.7$ lattice and the lower defect production at this composition[24] may well be related.

The buildup and the reconstruction of the damage induced by In ion implantation in various x $Hg_{1-x}Cd_xTe$, was studied in the present work by Rutherford backscattering spectrometry, and has been related to the nature of the bonds and to some mechanical properties of the alloy. However, only cross sectional TEM experiments on samples of different compositions implanted at doses corresponding to the three distinct regions (Fig. 3) can confirm the explanation offered in the present work.

ACKNOWLEDGMENTS

This work was supported by the U.S. Army (Contract No. DAJA45-86-C-001). The authors thank Dr. A. Muranevitch who has kindly furnished part of the samples.

[1] R. K. Willardson and A. C. Beer, *Semiconductors and Semimetals* (Academic, New York, 1981), Vol. 18.
[2] M. Roger, T. Brossat, P. Fragnon, J. Meslage, O. Pichard, and T. Nguyen Duy, Ann. Telecommun. 38, 62 (1983).
[3] P. Siffert, Rev. Phys. Appl. 12, 105 (1977).
[4] L. O. Bubulac, W. E. Tennant, S. H. Shin, C. C. Wang, M. Lanir, E. R. Gertner, and E. D. Marshall, Jpn. J. Appl. Phys. 19, 495 (1980).
[5] G. L. Destefanis, Nucl. Instrum. Methods 209/210, 567 (1983).
[6] S. Margalit, Y. Nemirovsky, and I. Rotstein, J. Appl. Phys. 50, 6386 (1979).
[7] J. Baars, A. Hurrle, W. Rothemund, C.R. Fritzsche, and T. Jakobus, J. Appl. Phys. 53, 1461 (1982).
[8] G. L. Destefanis, J. Vac. Sci. Technol. A 3,171 (1985).
[9] I. K. Volopyanov, S. P. Kozyrev, and A. V. Spitsyn. Sov. Phys. Semicond. 16, 626 (1982).
[10] C. Uzan, Y. Marfaing, R. Legros, R. Kalish, and Y. Richter, J. Cryst. Growth 86, 744 (1988).
[11] A. Sher, A. B. Chen, W. E. Spicer and C. K. Shih, J. Vac. Sci. Technol. A 3, 105 (1985).
[12] A. B. Chen, A. Sher, and W. E. Spicer, J. Vac. Sci. Technol. A 1, 1674 (1983).
[13] J. C. Phillips, *Bonds and Bands in Semiconductors* (Academic, New York, 1973).
[14] R. Triboulet, T. Nguyen Duy, and A. Durand, J. Vac. Sci. Technol. A 3, 95 (1983).
[15] N. R. Kyle, J. Electrochem. Soc. 118, 1790 (1971).
[16] K. Takita, T. Ipposhi, K. Murakami, K. Masuda, H. Kudo, and O. Seki, Appl. Phys. Lett. 48, 852 (1986).
[17] O. Dahir and R. Kalish, J. Appl. Phys. 54, 3129 (1983).
[18] L. C. Feldman and J. C. Rodgers, J. Appl. Phys. 41, 3776 (1970).
[19] P. F. Pronko, Nucl. Instrum. Methods 132, 249 (1976).
[20] S. T. Picraux, E. Rimini, O. Fot, and O. U. Campisano, Phys. Rev. B 18, 2078 (1978).
[21] Y. Quéré, J. Nucl. Mater. 53, 262 (1974); Radiat. Eff. 28, 253 (1976).
[22] T. M. Kao, Ph D. thesis, Stanford University, 1987.
[23] F. Bailly, in *Proceedings of Lattice Defects in Semiconductors*, edited by R. R. Hasiguti (University of Tokyo, Tokyo and Pennsylvania State University, Pennsylvania, 1968).
[24] S. Cole, M. Brown, and A. F. W. Willoughby, J. Mater. Sci. 17, 2061 (1982).

A METHOD FOR RAPID THERMAL ANNEALING OF COMPOUND SEMICONDUCTORS BY CW CO_2 LASER IRRADIATION

U. META, Y. RICHTER and R. KALISH
Solid State Institute Technion-Israel Institute of Technology
HAIFA ISRAEL 32000

ABSTRACT

A new Rapid Thermal Processing technique based on heating by irradiation from CO_2 laser is presented. It is particularly suitable for thermal treatment of low melting temperature materials such as annealing implantation induced damage in compound semiconductors.

Short time heating of the sample is achieved by its contact with a quartz plate heated by photons from a CW CO_2 laser. The quartz serves both as an absorbing medium for the radiation and as a proximity cap. Steady state temperature can be obtained by the simultaneous heating of the sample by the laser and its cooling by a jet of N_2 gas.

The present technique, when applied to ion implanted InSb (T_A<450°C, t=10 seconds), leads to removal of the implantation damage which is comparable to that obtained by furnace or flash lamp (Heatpulse™) annealing.

INTRODUCTION

Short time thermal treatment for the annealing of implantation induced damage has been extensively studied in recent years [1-2]. It has been shown to be particularly attractive in the case of low energy implantation into Si for shallow junction fabrication as dopant diffusion could be kept to a minimum by applying this technique. Rapid Thermal Annealing (RTA) has also been used on compound semiconductors, the most studied material being GaAs. Much less has been published on the rapid annealing of narrow band gap semiconductors such as InSb and $Hg_{1-x}Cd_xTe$. The main problem being the low melting point of these materials and hence the requirement for fairly low temperature (300-400°C) treatment. Nevertheless, the same arguments which make RTA attractive for the annealing of shallow implants in Si should also apply to compound semiconductors. Here too, diffusion processes which may accompany defect removal need to be avoided as much as possible. The major undesired diffusion in the case of the compounds is that of the more volatile constituents of the crystal, the loss of which leads to changes in stoichiometry and thus to changes in material properties. Previous work, mostly on RTA of $Hg_{1-x}Cd_xTe$, has indeed shown that defects could be removed with negligible changes in stoichiometry. In these studies encapsulated samples were heated either by short term exposure to light delivered by flash lamps [3-4], or by irradiation by photons from CO_2 lasers [5-7]. CdS caps were normally used in these studies to suppress Hg evaporation from the surface.

In the present work we report on the extention of the CO_2 laser annealing which we have developed for $Hg_{1-x}Cd_xTe$ studies. We describe an improved laser annealing arrangement, which permits capless annealing of the samples utilising the high absorption of quartz for 10.6 micron radiation and the indirect heating of the sample by its contact with the laser heated quartz plate. We show that good annealing can be achieved with this arrangement also for ion implanted InSb. The annealing quality, as determined from RBS channeling experiments, is shown to be comparable to that obtainable by furnace or by flash lamp (Heatpulse™) heating.

EXPERIMENT AND RESULTS

The CO_2 laser and its beam transport are shown in figure 1 together with the temperature control feedback arrangements. Radiation from a powerful CW CO_2 laser (maximum power 1.5 kW operated for this experiment at only 300 W), with a computer controlled shutter, is focused by a 3.75" ZnSe lens into a beam homogenizer consisting of a simple rectangular cavity made out of 4 polished stainless steel plates. The beam emerging from this homogenizer is uniform over its 1x1 cm^2 apperature, with only fine regularly spaced slight variations in intensity noticable on exposed photographic paper. This inhomogeneity depends on the relative distance between the lens, the homogenizer and the sample, and it can be minimized by appropriate choice of these parameters. It is however of no importance to the present annealing procedure, since temperature uniformity on the sample surface is achieved in the quartz diffuser, as will be described below. The sample arrangement is shown in detail in figure 2. It consists of the sample sandwiched between two quartz plates, the bottom one with a thermocouple glued into a hole in its center. The top quartz plate serves as an absorbing medium for the 10.6 micron radiation from the CO_2 laser, a temperature diffuser, and as a proximity cap for the sample. The temperature of this top plate is monitored by a pyroelectric detector (manufactured by "GALAI") which is sensitive to the relevant temperature range (200-700°C). The temperature readings as a function of time for both thermocouple and pyroelectric detector are monitored. Any one of them can be used to automatically open a solenoid valve which permits a stream of N_2 gas to flood the sample, thus cooling it when a desired preset temperature is reached. A constant sample temperature can be maintained in this way. Representative time-temperature curves for short time and for longer (steady state) heating are shown in figure 3. It should be noted that when higher laser powers were used, temperatures up to 1300°C could be reached by this arrangement, within 5 seconds from the start of the laser pulse. Thus the same arrangement was also used by us for RTA of ion implanted Si.

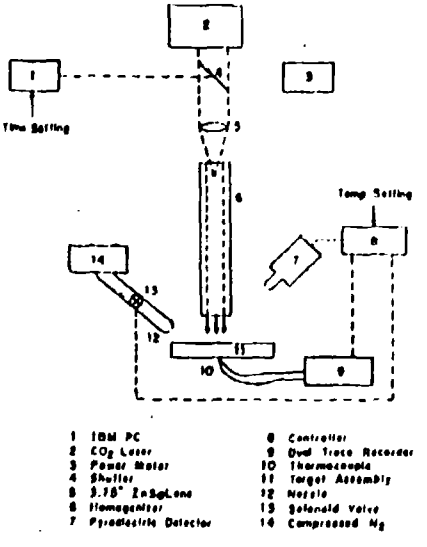

fig.1 Experimental arrangement used for the CO_2 laser annealing

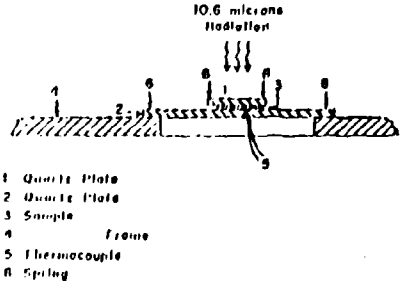

fig.2 Sample assembly

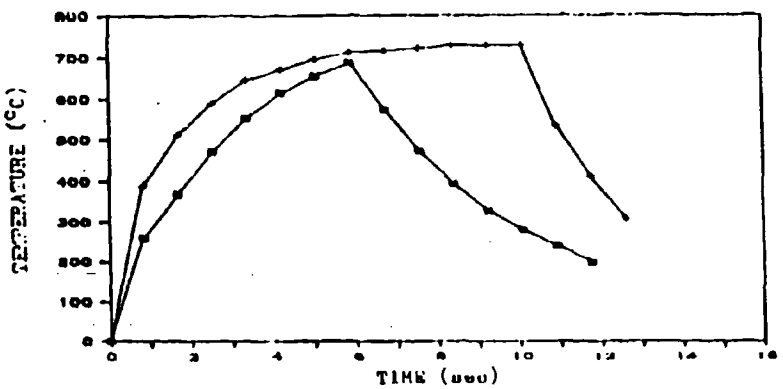

fig.3 Time-temperature curves as measured with the pyroelectric detector, viewing the top quartz plate: square-direct laser heating and crosses- heating with N_2 jet cooling.

Indium Antimonide <111> oriented crystals were implanted, at room temperature, with Zn ions to a dose of $1x10^{13}cm^{-2}$. The samples have been exposed to short time heating obtained by either CO_2 laser arrangement by light flashes from the Heatpulse™ or to a furnace annealing of 400 °C for 30 minutes. Temperature was varied for both cases in the range of 300-400 °C with nominal heating times kept at either 5 or 10 seconds. Samples for the furnace annealing were encapsulated with evaporated 500Å SiO_2. This layer was chemically removed after annealing.

The sample quality before and after annealing was studied by performing Rutherford Backscattering (RBS) channeling experiments with 320 keV protons. Representative results are shown in figure 4 where the spectra of the channeled protons scattered at an angle of 165° are shown following both CO_2 laser and Heatpulse™ (t=10 sec, T=400°C) annealing. Also displayed are the spectra measured for the virgin and as implanted samples as well as a random spectrum. The as implanted spectrum shows no damage peak, instead the implantation induced damage reflects itself through the dechanneling of the probing beam.

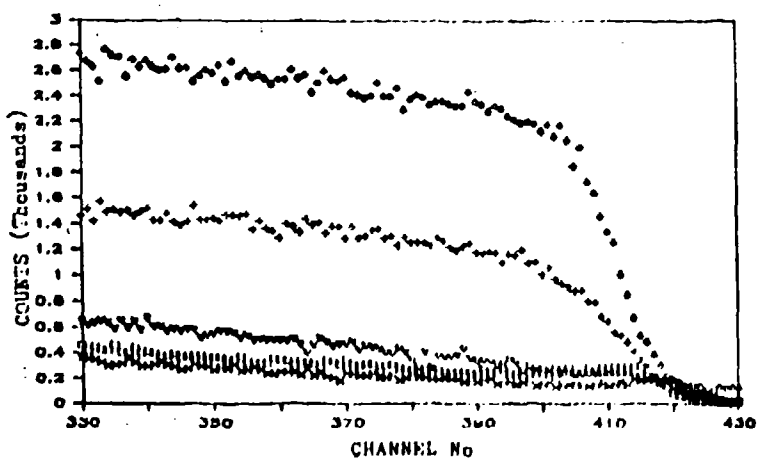

fig.4 Channeled RBS spectra for: virgin-(x); as implanted-(+); laser annealed 400°C;10sec.-(▽); Heatpulse annealed 400°C;10sec.-(□); random-(◇).

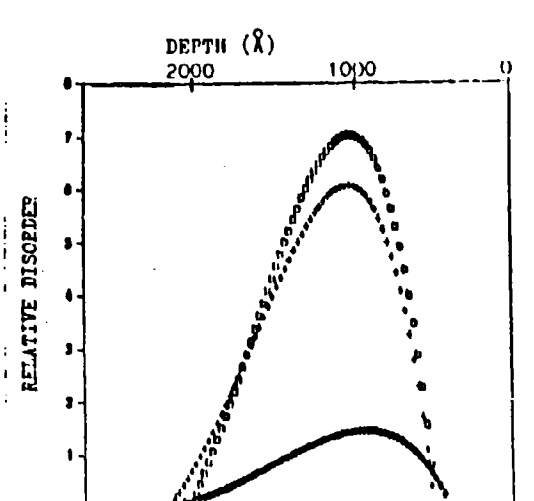

Fig.5 Damage profile as a function of depth as deduced (ref. 8) from the dechannelling for different annealing temperatures: squares-as implanted; crosses-280°C:10sec; diamond- 320°C:10sec.

The damage created in InSb crystals by the implantation is comprised mainly of extended defects. As can be seen from the spectra, good annealing could be obtained for both techniques when the sample has been exposed to 400°C for 10 seconds. The damage profile has been deduced from the dechannelling of the protons by the procedure described by Feldman and Rodgers [8]. Those net profiles are shown in figure 5. In order to check whether the annealing has caused major changes in the near surface stoichiometry, Auger Electron Spectroscopy depth profiling was carried out. The results of such measurments are shown in figure 6. As can be seen from this figure only the topmost 200Å have been affected by the annealing procedure.

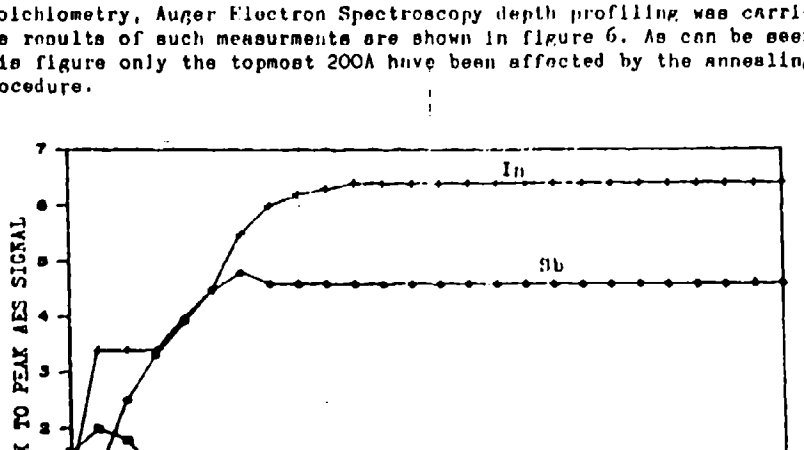

fig.6 Auger Electron Spectroscopy for CO_2 laser annealed sample (T=400°C:10sec.) showing oxidation and stoichiometry changes extending to about 200Å from the surface

DISCUSSION

The new method for short time thermal processing described here, which relies on indirect heating by irradiation from a CW CO_2 laser, has several attractive features. Powerful CO_2 lasers are readily available, and offer an inexpensive way to convey heat through windows which are transparent to the 10.6 micron radiation to the sample. It can therefore be easily applied to samples kept at various atmospheres in simple glass container. The use of the thermal mediator is simple, ensures lateral thermal uniformity over the sample and it may serve as a proximity cap to supress the loss of volatile constituents of the crystal. The fact that the heat is transfered to the sample through its contact with an absorbing medium opens interesting avenues for research on the role that the direction of heat flow has on the quality of the annealing. In contrast to heating in a furnace or in the Heatpulse™ instrument, where the sample is placed inside a hot cavity and is heated simultaneously from all directions, here the heat flows through the sample from the surface which faces the laser. This face can be the implanted surface or the opposite one, hence annealing quality with the heat flowing through the implanted region into the bulk of the crystal, or from inside the crystal to the damage crystal-interface and then to the surface can be studied. InSb is a good candidate for such studies because of its poor thermal conductivity so that an appreciable temperature gradient across the sample is expected. We have attempted such measurments, in which we have looked for the dependence of annealing quality on irradiation direction, but have no conclusive results yet. The main difficulty being how to ensure that the temperature at the implanted layer is the same for both irradiation directions. The quartz mediator is, of course, not essential for the present technique. A deposited SiO_2 layer on top of the sample will serve the same purpose of absorbing the 10.6 micron radiation from the CO_2 laser (the absorption coefficient for SiO_2 is 10^4 cm^{-1}) and transfering it into the crystal. It too will serve as a protective cap, however, with the disadvantages related to difficulties in deposition and removal of the film. As we have mentioned above, the technique is not necessarily limited to low temperature thermal treatment, and we have also demonstrated its usefulness to implanted Si, however the high thermal stress involved in unidirectional high gradient heating will probably be undesirable due to the high internal stress which must accompany it.

The described method needs refinement mainly in two points: a) The determination of the real temperature at the implanted surface is problematic as it depends on the thermal contact between the quartz plate and the sample, and b) The annealing reproducibility is hard to obtain because of inherent variation in laser output. The first problem can be avoided by the use of an absorbing material deposited on the sample surface or by performing reliable heat transport calculations and assuring reproducible good contact between the surfaces. The second can be overcome by careful and repetitive adjustment of the laser operating conditions.

ACKNOLEDGEMENTS

We wish to thank Dr. G. Laufer and Mr. Y. Barzilai for assistance in the laser treatment, Mr. A. Katz for help with the Heatpulse™ annealing and Dr. R. Brener for the Auger analysis. This work supported in part by the US Army ERO contract DAJA45-86-C-0011.

REFERENCES

1. Poate, J.M., and Mayer, J.W., "Laser and Electron Beam Processing of Semiconductor Structures" (Academic Press,New York,1982).

2. J. Narayan and O. W. Holland, J. Appl. Phys. 56 (10), 2913 (1984).

3. C. Uzan, Y. Marfaing ,R. Kalish and V.Richter "Properties of In and Ar Implanted $Hg_{0.3}Cd_{0.7}Te$ Following Furnace and Rapid Thermal Annealing" (to be published in J. Appl. Phys.)

4. C. Uzan, R. Kalish, V. Richter and T. Nguen Duy, SPIE Vol.659; Materials Technologies for IR Detectors (1986) p. 81.

5. G. Dahir and R. Kalish, J. Appl. Phys. 54, 3129 (1983).

6. G. Dahir, R. Kalish and Y. Nemirovski, Appl Phys. Lett. 41, 1057 (1982).

7. R. Kalish and G. Dahir, J. of Cryst. Growth 72, 474 (1985).

8. J. C. Feldman and J. W. Rodgers J. Appl. Phys. 41, 3776 (1970).

Rapid annealing of $Hg_{1-x}Cd_xTe$ by immersion in a hot mercury bath

R. Kalish, R. Fastow, V. Richter, and M. Shaanan
Solid State Institute, Technion, Israel Institute of Technology, Haifa 32000, Israel

(Received 16 June 1987; accepted for publication 13 August 1987)

A simple technique for annealing ion implanted $Hg_{1-x}Cd_xTe$ in a mercury atmosphere has been developed. In this technique, $Hg_{1-x}Cd_xTe$ is sandwiched between two silicon wafers and immersed in a hot mercury bath. This permits rapid annealing at well defined temperatures and times. Indium-implanted $Hg_{1-x}Cd_xTe$ ($x = 0.23$ and $x = 0.7$) samples have been annealed using this method at temperatures ranging from 260 to 350 °C and for times ranging from 3 s to 1 h. The near surface crystalline quality, as measured by ion channeling, improved after annealing and was comparable to that obtained by other annealing techniques. No change in surface stoichiometry, as measured by particle-induced x-ray emission, was detected in the $Hg_{0.77}Cd_{0.23}Te$ samples.

The doping of HgCdTe by ion implantation relies on the n^+ layer formed as a result of implantation damage, rather than on the activation of the dopant atoms. By relying on the damage produced during implantation, many of the advantages that ion beam implantation offer are lost (i.e., control of the junction depth and the doping level). Attempts at annealing HgCdTe have been complicated by the loss of mercury which occurs during even moderate heating in a vacuum or in an inert atmosphere. Published values for the loss rate of mercury as a function of annealing time and temperature predict an almost complete depletion in the top few hundred angstroms following a 1-min anneal at 350 °C.[1] Since mercury vacancies act as acceptors in *n*-type material,[2] a loss of 10^{16} Hg/cm^3 is usually enough to convert the semiconductor surface from *n* type to *p* type. Therefore, capping layers, annealing in a mercury atmosphere, or rapid annealing with incoherent light sources or cw lasers, have been attempted.[3–6] Crystalline quality has been found to improve with all of the above methods. Realization of a *p*-on-*n* photodiode by the partial activation of *p*-type dopants has been reported following short duration CO_2 laser annealing[7]; and successful *p*-type dopant activation after capped furnace annealing has also been reported, indicating that the damage-related *n*-type activity was removed.[8] In the present work, we have developed a new technique to anneal ion implanted $Hg_{1-x}Cd_xTe$, with the objective of removing the implantation-induced damage without altering the surface stoichiometry. The advantages of this capless annealing technique are its simplicity and the possibility for short time anneals (~ 1 s) with accurate time and temperature control.

Single crystals of $Hg_{0.77}Cd_{0.23}Te$ and $Hg_{0.30}Cd_{0.70}Te$ oriented in the (111) direction were mechanically polished and etched in a bromine-methanol solution prior to ion implantation. Implantation of 300 keV In^+ ions at a dose of 1×10^{14}/cm^2 was carried out at room temperature. To avoid sample heating, the current density of the beam was kept below 0.1 μA/cm^2. The projected range and straggling for such implantations are 850 and 450 Å, respectively. During implantation, half of each sample was covered for later comparison and for the evaluation of the effects of thermal treatments on unimplanted material. Annealing, following implantation, was carried out in a newly designed apparatus which is sketched in Fig. 1. A Pyrex flask, partially filled with pure mercury, was heated to 260–350 °C. The temperature was measured by immersing a mercury thermometer into the bath, and vapors were prevented from escaping by attaching a water-cooled condenser to the top of the flask. The HgCdTe sample, sandwiched between two polished silicon wafers, was lowered into the mercury bath for the desired annealing times. As mercury does not wet the surfaces of either HgCdTe or silicon, it could not enter the small gaps between the wafers. Hence, liquid mercury never came into direct contact with the HgCdTe surface, yet a mercury overpressure at the surface was maintained. Since the bath temperature was accurately measured, as was the dipping time, rapid annealing at well defined temperatures and times was possible. Because of the high thermal conductivity of liquid mercury and the small heat capacity of the sample assembly, a nearly instantaneous temperature rise (less than 100 ms) to the temperature of the bath could be achieved.

Samples were immersion annealed for times ranging from 3 s to 1 h at temperatures from 260 to 350 °C. The reduction of defects as a result of thermal treatment was evaluated by ion channeling in the (111) direction using 320

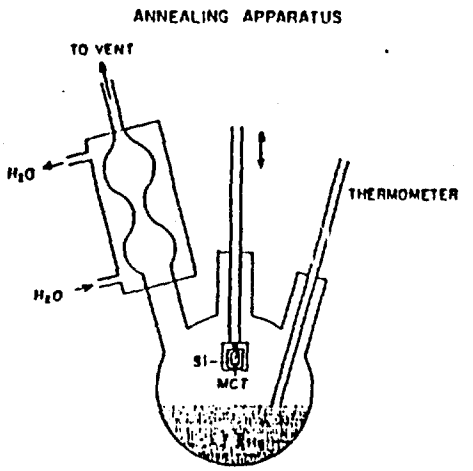

FIG. 1. Apparatus for the rapid thermal annealing of $Hg_{1-x}Cd_xTe$ in a mercury atmosphere.

 0003-6951/87/411158-03$01.00

keV protons. Figure 2 shows a typical set of channeling spectra before and after annealing $Hg_{0.77}Cd_{0.23}Te$ for 30 s at various temperatures. Random and channeled spectra for a virgin crystal are also shown. The quality of the unimplanted sample can be determined from the ratio of the channeled virgin spectrum to the random virgin spectrum at the surface (χ_{min}). Spectra 2(a) and 2(b) yield a value for χ_{min} of 10.5%. Implantation of indium results in a gradual dechanneling which is typical for damage in $Hg_{0.77}Cd_{0.23}Te$ [spectrum 2(c)]. The width of this dechanneling region indicates that extended defects are present to a depth of 2700 Å, which is three times the projected ion range. The effects of thermal treatment on the implanted sample are shown in spectra 2(d) and 2(e), corresponding to annealing temperatures of 260 and 350 °C, respectively. Both of these spectra are comparable to those obtained by other rapid annealing techniques. Channeling spectra from the unimplanted region remained the same after annealing.

The near surface stoichiometry of HgCdTe was determined by measuring the characteristic x rays excited by low-energy protons (PIXE). To the first order, changes in the x-ray yields were proportional to changes in the relative amounts of Hg, Cd, and Te. A PIXE spectrum taken from a $Hg_{0.77}Cd_{0.23}Te$ sample after annealing for 30 s at 280 °C is shown in Fig. 3. The peaks corresponding to the *L* groups of Cd and Te, and the *M* group of Hg are well resolved. This spectrum was taken with 340 keV protons which probe an effective depth of 3600 Å. A number of spectra were taken with different proton energies in order to probe the composition at various depths. These data are represented in Fig. 4 where the ratios of the Hg to Te x-ray yields are plotted as a function of energy for both the virgin and annealed samples. The fact that these yields are nearly identical indicates that the surface stoichiometry remained constant to within the statistical error of ± 3%. The relationship between proton energy and effective depth is also shown in Fig. 4, and was calculated by taking into account the proton energy loss and x-ray ionization cross sections as a function of energy, and

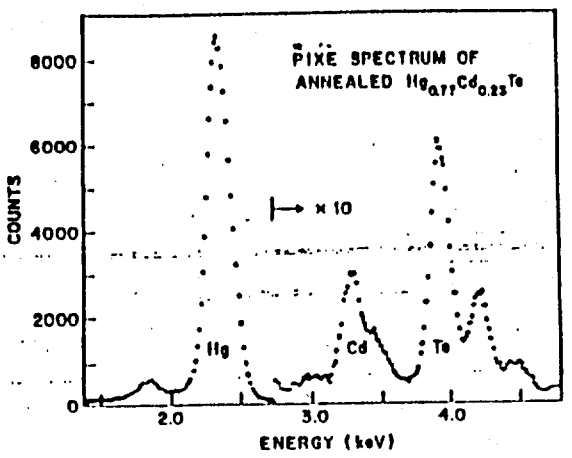

FIG. 3. Particle-induced x-ray spectra, taken with 200 keV protons, of $Hg_{0.77}Cd_{0.23}Te$ after annealing for 30 s at 260 °C.

the x-ray attenuation factor as a function of depth. Since the mean depths probed at a given energy are slightly different for each element, the effective depth was defined as the average of the three mean depths. PIXE measurements taken on $Hg_{0.30}Cd_{0.70}Te$ before and after annealing for 5 min at 310 °C clearly showed excess mercury extending thousands of angstroms into the crystal. It is not clear at the present time whether this penetration was due to the much longer annealing time and higher temperature, the differing sample stoichiometry, or other basic differences between the crystals.

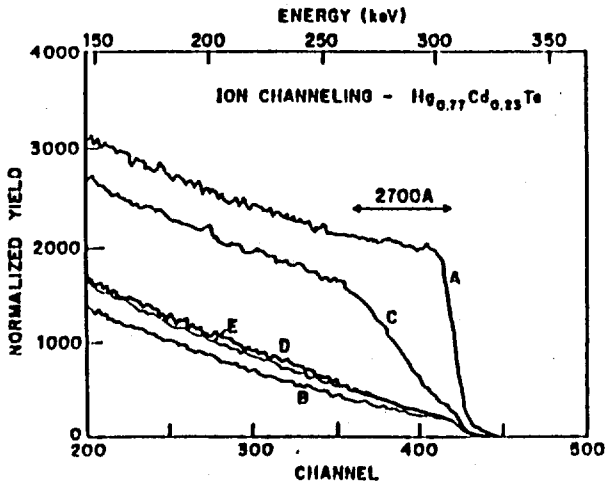

FIG. 2. Ion channeling spectra of $Hg_{0.77}Cd_{0.23}Te$: (a) virgin, random direction; (b) virgin, aligned direction; (c) implanted, unannealed; (d) implanted, annealed for 30 s at 260 °C; (e) implanted, annealed for 30 s at 350 °C.

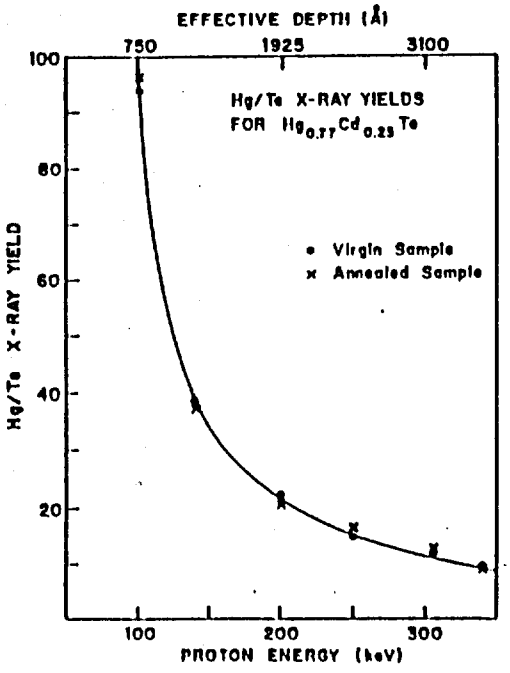

FIG. 4. Ratio of the mercury to tellurium x-ray yields for $Hg_{0.77}Cd_{0.23}Te$ before and after annealing for 30 s at 260 °C. The PIXE yields are plotted as a function of the incident proton energy. The curve through the data points is to guide the eye.

Optical micrographs of the surface taken before and after annealing showed that good surface morphology was maintained. The surface of the annealed sample remained smooth, although a low density ($\sim 1000/cm^2$) of pits 2–3 μm in diameter was observed. It is probable that the pitting was caused by condensation of mercury vapor on the surface.

In summary, we describe a new and simple apparatus for annealing HgCdTe. The advantages of this technique are that short time (~ 1 s) capless anneals in a mercury atmosphere at well defined temperatures and times are possible. It was demonstrated that immersion annealing can restore the crystallinity of indium implanted $Hg_{0.77}Cd_{0.23}Te$, maintain the near surface stoichiometry, and preserve the surface morphology.

The authors would like to thank C. Uzan for many helpful discussions. One of us (R. Fastow) acknowledges the support of The Lady Davis Fellowship Trust. This research was supported by the U.S. Army (contract No. DAJA45-86-C-0011).

[1] K. C. Dimiduk, W. G. Opyd, J. F. Gibbons, T. W. Sigmon, T. J. Magee, and R. D. Ormond, J. Vac. Sci. Technol. A 1, 1661 (1983).
[2] C. L. Jones, M. J. T. Quelch, P. Capper, and J. J. Gosney, J. Appl. Phys. 53, 9080 (1982).
[3] G. Dahir, R. Kalish, and Y. Nemirovsky, Appl. Phys. Lett. 41, 1057 (1982).
[4] T.-M Kao and T. W. Sigmon, Appl. Phys. Lett. 49, 464 (1986).
[5] J. Baars, A. Burrle, W. Rothemund, C. R. Fritzche, and T. Jakobus, J. Appl. Phys. 53, 1461 (1982).
[6] K. L. Conway, W. G. Opyd, J. F. Gibbons, and T. W. Sigmon, Nucl. Instrum. Methods 209/210, 651 (1983).
[7] R. Kalish and G. Dahir, J. Cryst. Growth 72, 474 (1985).
[8] H. Ryssel, G. Lang, J. P. Biersack, K. Muller, and W. Kruger, IEEE Trans. Electron Devices ED-27, 58 (1980).